Reply to Reviewer2

We do appreciate the reviewer provide so much important comments help us improving our manuscript. We'd like to address these comments as following.

Line 2: "that require a whole volume radar data" should read as…. "that require a whole volume of radar data"
Response: the manuscript was modified following the reviewer's comment.

Line 7: "with multiple precipitation events including two widespread mixture of stratiform and convective events" May read better as….. with multiple precipitation events including two widespread mixed stratiform and convective events"
Response: the manuscript was modified following the reviewer's comment.

line 10: "can accurately identify the convective cells from stratiform storms with the radar data only from the lowest scan in tilt. It can produce better results than using the separation index only." Would read better as……. "can accurately identify the convective cells from stratiform rain using radar data from the lowest scan in tilt only, and produced better results than using the separation index only."
Response: the manuscript was modified following the reviewer's comment.

Line 15: "convective precipitation's are associated with" reads better as …convective precipitation is associated with"
Response: the manuscript was modified following the reviewer's comment.

line 16: "while stratiform precipitations are associated" reads better as……while stratiform precipitation is associated"
Response: the manuscript was modified following the reviewer's comment.

line 17: what is meant by saying a convective system consists of large and dense raindrops?
Response: It was found the values of raindrop's mass weighted mean diameter(Dm) in stratiform and convective precipitation generally are within 1-1.9 mm and above 1.9 mm, respectively (Chang et al., 2009). Following the review's comment, we added more discussions in the manuscript L:80~83

Line 53: "of the DSD-based approaches depends on the environmental regime"….Could you expand upon this a little bit please?
Response: The separation index derived from Equations 2~5 in the manuscript depends on several factors: the radar wavelength, temperature, drops size distribution(DSD), and drop shape relations(DSR). The last three factors depend on environmental regime. In our work, we demonstrated that temperature, DSD and DSR features from Taiwan very similar to Darwin, Australia. Therefore, all the coefficients derived by BAL can be directly used in the current work. Following the review's comment, we added more discussions in the manuscript L:123~135.

Line 58 and 59: "classification results even it is operated"…… Reads better as…. classification results even if it is operated"

Response: the manuscript was modified following the reviewer's comment.

line 68: "together with other three single polarization"….Reads better as… together with the other three single polarization"

Response: the manuscript was modified following the reviewer's comment.

line 73: "for convective and stratiform precipitations, total 4306 minutes of DSD data"….Reads better as…… for convective and stratiform precipitation, a total of 4306 minutes of DSD data"

Response: the manuscript was modified following the reviewer's comment.

line 81: "stratiform precipitations generally consist of condense of small to median raindrops"….. This sentence needs to be corrected and explained better.

Response: this sentence is modified as in L:80-83.

Line 98: "using the separation index i to identify convective precipitation from stratiform" … This may read better as ..using the separation index i to identify convective from stratiform precipitation"

Response: the manuscript was modified following the reviewer's comment.

Line 100: I assume that Nw refers to liquid water concentration… Is this true?

Response: N_w is the normalized number concentration in the gamma drop size distribution.

Equation 5: it may help to list as equations 5a) and 5b)

Response: the manuscript was modified following the reviewer's comment.

Lines 157 – 160: I understand the authors using the MRMS precipitation classification algorithm as ground truth….However, he should be noted that there are many imperfections in the system, especially since it only uses single pole information to determine echo classes

Response: We appreciate the reviewer point this out.

In the revision, we made the following statements in the revision L:170~181:

"Thirdly, the precipitation type is confirmed by the Multi-Radar-Multi-Sensor (MRMS) precipitation classification algorithm implemented in Taiwan (Zhang et al., 2011, 2016). In this MRMS classification approach, a three-dimensional radar reflectivity field was mosaicked from 4 S-band single-polarization radars (Figure 1). The composite reflectivity (CREF) and other measurement such as temperature and moisture fields were then used in the surface precipitation clas- sification (Zhang et al., 2016). Based on the classification results, MRMS chooses different $R(Z)$ relations in the rainfall rate estimation. The performance of MRMS has been thoroughly evaluated for years for the quantitative precipitation estimation, flash flood monitoring, severe weather, and aviation weather surveillance (e.g., Gourley et al., 2016; Smith et al., 2016). The products are used as the benchmark and ground truth in many studies

(e.g., Grecu et al., 2016; Skofronick-Jackson and Coauthors, 2017). It should be noted that, on the other hand, the MRMS also shows limitations since it only uses single-polarization variables to determine the precipitation type. At the current stage, the MRMS precipitation classification is considered as the appropriate benchmark in the training and validation of the proposed algorithm. Moreover, since the MRMS classification is a mosaicked product derived from 4 S-band radars, it can be viewed as an independent reference."

Line 165: "total one hour data were used as the convective type training data in the training data are associated with the >20 dBZs"….. What is meant by "total one hour data"?
Response: The radar data collected from 1030 UTC to 1130 UTC are used in the training. Given the radar VCP, there are total 13 volume scans data are available.

Line 169: " the number of support vectors is selected as 1000 and the current work"….Not everyone who reads this article will be familiar with some of the machine learning/artificial intelligence setting of criteria… It may help to add a few more lines on this… You have done that in lines 170 through 172 but still it would help to go a little bit further into what is typically done for these types of learning algorithms.
Response: We do appreciate the reviewer point this out. We added more discussion in the revised manuscript in L:192~200.

Line 188: "results from RCMK……and MRMS could be different as large as five minutes in time stamps"…… This may read better if written as .. results from RCMK……and MRMS could be significantly different with timestamp differences as large as five minutes"
Response: the manuscript was modified following the reviewer's comment.

line 190: "evaluation criteria of the possibility of detection" … Should read as evaluation criteria of the probability of detection"
Response: the manuscript was modified following the reviewer's comment.

line 197: "was first validated with two widespread mixture of stratiform and convective"…… Should read as… was first validated with two widespread stratiform and convective mixed"
Response: the manuscript was modified following the reviewer's comment.

Line 241: "it could found that the heavy precipitation band"… Should read as .. it was found that the heavy precipitation band"
Response: the manuscript was modified following the reviewer's comment.

Line 253: "different from some existing classification algorithms" would read better as "different from other classification algorithms"
Response: the manuscript was modified following the reviewer's comment.

Lines 273 – 274: "second, the performance of the proposed approach highly depends on the training data. It should be very careful to select the training data." This would read better as

“second, the performance of the proposed approach depends highly on the training data which should be very carefully selected. “

Response: the manuscript was modified following the reviewer’s comment.

Reply to Referee 3

We do appreciate the reviewer provide so much important comments help us improving our manuscript. We'd like to address these comments as following.

1.) First of all, an important comment the proposed methodology, which uses the lowest unblocked scanning tilt, as stated by the authors at page 2 (Line 55). In my opinion, the authors should add a discussion about the weakness of such approach, considering, for example, the scenario in which it is applied in a complex-orography area. In such a case, the strategy may be not suitable, because the radar signal at lowest tilt may be totally or partially obstructed by the surrounding topography in some sectors. A possible solution to overcome this issue may be using the lower "free" available scanning elevation but this choice can generate inconsistencies and biases. For example, in some sectors of radar coverage, the algorithm may receive as input the reflectivity data collected at 1° elevation, in others the measurements sampled at 4° antenna elevation angle. The information provided by data sampled at 1° and 4° antenna elevation angle can be very different, depending on the precipitation type event that is taking place.

Response: Thank you for the reviewer pointing this out. First, we totally agree with the reviewer that a discussion about the weakness of the proposed approach is necessary, which can guide readers to evaluate and implement this approach. We added following discussion in the revised manuscript:

1.) **Line 56**: Different from some existing classification techniques that require whole volume scan of radar data, this new approach uses the lowest unblocked tilt data in the separation. If the lowest tilt is partially or completely blocked, then next adjacent unblocked tilt is used instead.
2.) **Line 336**: Limitations of proposed approach are also included in the discussion section as: First, this approach is developed for fast scanning and fast update purpose, therefore, data from the lowest unblocked tilt is used as the input. However, if the radar is located in a complex orography area, radar beam could be partially or completely blocked at some regions. A possible solution for such scenario is using a hybrid scan data from different scanning tilts as the input. Radar scanning tilts used in the hybrid scanning are determined by the radar scanning geometry**.** Given the factor that precipitation's microphysics (such as drop size distribution) from different altitudes may be significantly different, therefore, the performance of proposed approach may worse than expected.

Secondly, the data from 1.4° elevation angle is used in the current work. Following figures show the scanning geometry of RCMK, and this figure was also added in the manuscript as the reviewer suggested. From this figure, we can find that the data from 0.5° is severely blocked by the central mountain range. Therefore, data from 1.4° elevation angle (treated as lowest unblocked data) is used in the current work.

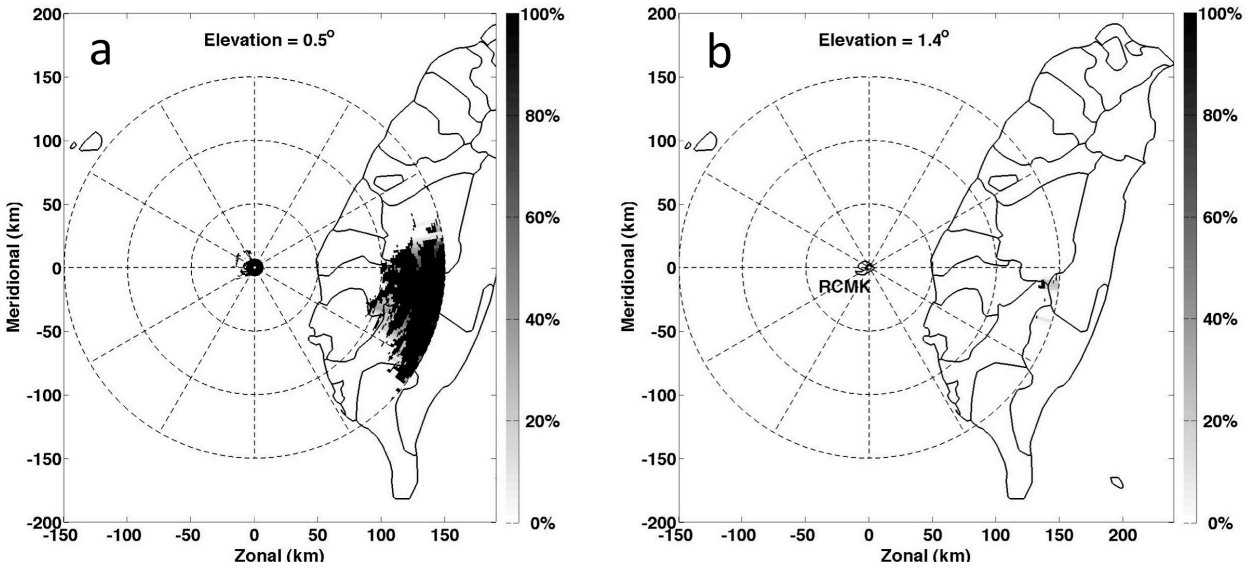

Figure 1. Blockage maps of RCMK from the first 2 elevation angles (0.5° and 1.4°). The grey scale indicates the blockage percentages.

2.) In Section 2, I suggest to add a figure showing the scanning geometry of the C-band polarimetric radars involved in this study. Please indicate the elevations angles used to develop the SVM method. Moreover, it is not clear if the authors used also the measurements provided by S-band single-polarization systems operating in the area of Taiwan.

Response: Following the reviewer's suggestion, a figure of the scanning geometry of RCMK is added in the revised manuscript. The data from 1.4° elevation angle (the lowest unblocked tilt) is used in the algorithm development. We included this clarification in the revised manuscript. The S-band single-polarization radar data is not used in the SVM approach. We clarify this too in the revised manuscript.

3.) In Section 2, the authors describe the variables used as input to the SVM method. They discuss about quality control of reflectivity measurements, focusing only on a specific issue, the attenuation along the path. I suggest to extend this discussion to other radar impairments that may have a strong impact on the performance of the proposed methods, such as the ground clutter (which strongly affects the radar measurements quality at lowest tilt) and the reflectivity vertical profile. In this respect, a detailed discussion should be provided about the bright band, which is a typical signature of stratiform precipitation events.

Response: Following the reviewer's suggestion, issues about ground clutter and VPR are discussed in the revised manuscript. The discussion about bright band is also included as suggested.

Line 98: Other quality control issues, including calibration, reflectivity vertical profile, and

ground clutter removal, were also considered in this work. Since this radar is used in the real-time quantitative precipitation estimation, the biases of Z and Z_{DR} should be within 1 dBZ and 0.1 dB, respectively. The data quality of RCMK was examined through validating the QPE performance in different works (e.g., Wang et al., 2013, 2014). Therefore, the calibration bias of RCMK should be within a reasonable range. A vertical profile of reflectivity (VPR) correction is generally needed on the reflectivity field to reduce the measurement biases because of the melting layer (Zhang et al., 2011). Given the fact that 1.4° elevation angle is used within the maximum range of 150 km, and the melting layer is usually around 5 km in Taiwan, the radar data is well below the melting layer. In addition, considering the vertical profile of differential reflectivity is not well studied in the current stage, no vertical corrections are applied to fields of Z and Z_{DR}. Ground clutter is typically associated with a low correlation coefficient (ρ_{HV}), the ρ_{HV} threshold used in this work is 0.9, which can effectively remove those non-meteorological echoes such as ground clutter.

Line 163: On the other hand, stratiform precipitations are generally associated with a prominent bright band signature. The melting hydrometeors increase backscatter during stratiform rainfall, which can significantly enhance radar reflectivity. The bright band feature is one of the obvious indicators of stratiform precipitation. Bright band signature normally can be observed from relatively high EAs (such as above 9.9°). From low EAs, because of the combination of radar beam broadening and low slant angle, the bright band feature spreads into more gates and becomes not apparent. Therefore, in this work, the bright band feature from high elevation angles is only used in training data selection but not used as one of the inputs.

4.) Section 2.3, in my opinion, it may useful cite some previous work that developed machine-learning algorithm based on meteorological radar data. I suggest the following reference: Capozzi et al. (2018), Adity Sai Srinivas et al. (2019) and Yen et al. (2019).

Response: Following the reviewer's suggestion, these three references were added into the revised manuscript.

Line 139: Machine learning algorithms based on meteorological radar data were well developed during the past two decades (e.g., Capozzi et al., 2018; T. et al., 2019; Yen et al. 2019)

5.) As training data for convective precipitation type, the authors use the measurements collected in a single event occurred on 23 July 2014. More specifically, for this event radar data collected from 10:30 to 11:30 (one hour) were used. I am quite skeptical about this choice, that the authors must justify and explain. It is well note that convective events may be triggered by different meteorological scenarios and that may exhibit different features in radar data according to thunderstorm types (single cell, squall line, supercell, etc.).

Response: In this work, the training data plays a critical role in the SVM development. Therefore, we choose convective and strtiform precipitations following three major steps.

1.) First, the training data was checked following general classification principles: for example, heavy precipitation band associated with high reflectivity for convective type precipitation; bright band for stratiform type precipitation.
2.) Second, the ground observation is used as another reference. For example, the severe weather report could be used as the ground observation.
3.) The classification results from MRMS is used as the third reference.

The convective type precipitation data is mainly from a thunderstorm on 23 July 2014. An aircraft crash tragedy caused by strong downdraft is used as the ground observation. MRMS classification algorithm classifies this event as the convective precipitation type. The radar observation of reflectivity Z and differential reflectivity Z_{DR} at 0858 UTC is shown in Fig. 2

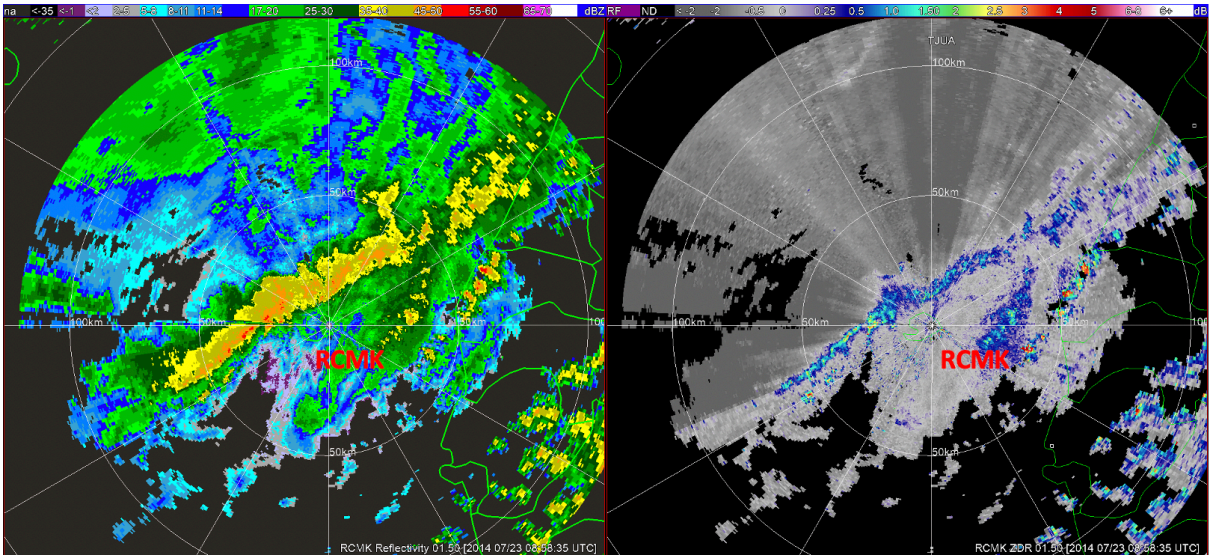

Figure 2. Reflectivity (left) and differential reflectivity (right) at 0858 UTC, 23 July 2014.

A clear squall line features can be identified at this moment, which triggered the strong updraft/downdraft. Inside this squall line, the reflectivity field is above 40 dB; differential reflectivity field is above 1 dB. The maximum value of Z_{DR} could be as high as 2.5 dB. Behind the severe precipitation band, the differential reflectivity field drops to negative value because of the attenuation issue. Fields of Z and Z_{DR} from 1028 UTC are shown in Fig. 3. Although the squall line signatures are not as well structed as 0858 at this moment, clear convective precipitation features such as large reflectivity, and very positive differential reflectivity are still very obvious. Therefore, we use those gates classified as convective type as in the training data.

We hope these plots can address the reviewer's concerns.

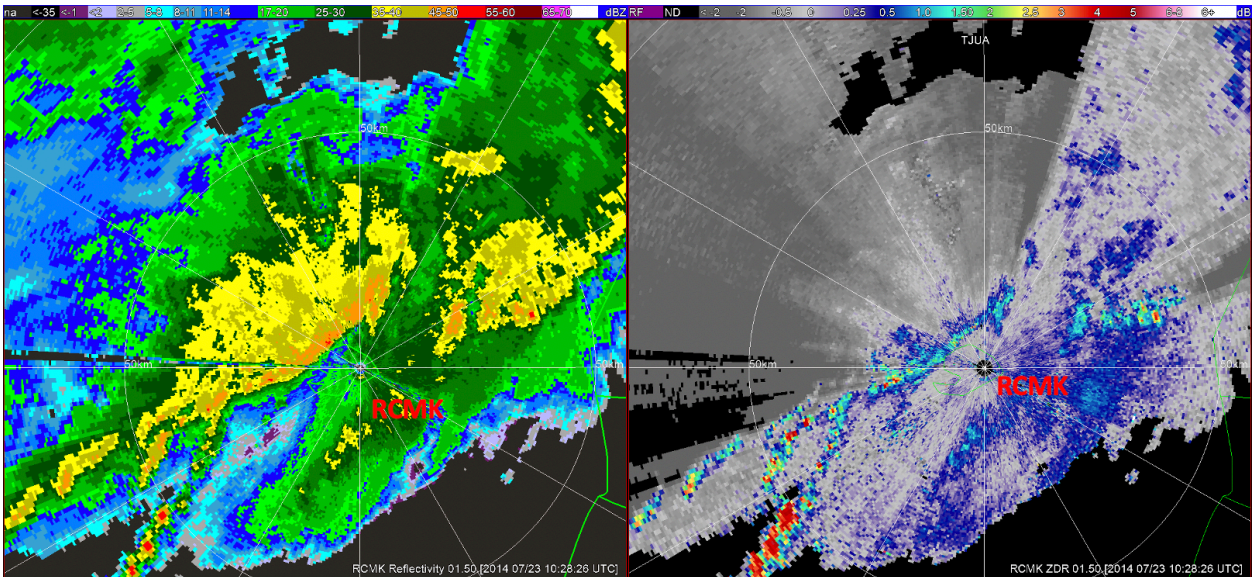

Figure 3. Reflectivity (left) and differential reflectivity (right) at 1028 UTC, 23 July 2014.

6.) Moreover, at page 6 (line 166) the authors declare that 17281 sets of data have been used in the training process. What does it mean "sets"? A clarification about this point is required.

Response: We appreciate the reviewer pointing this out. A "set" means a set of data from one radar gate (defined as azimuthal angle and range). Be more specific, a set of training data means a vector of $[Z(a,r)\ Z_{DR}(a,r)\ i(a,r); d(a,r)]$. Where "*a*" indicates azimuthal angle, "*r*" indicates range; "d" is the desired response with "1" represents convective, and "-1" represents stratiform.

Line 188: A total of 17281 sets of data (15144 sets of stratiform, and 2137 sets of convective) are used in the training process. In this work, one data set is defined as the variables from a single gate in terms of range and azimuthal angle. Be more specific, a collection of training data means a vector of [$Z(a, r)$ $Z_{DR}(a, r)$ $i(a, r)$ $d(a, r)$], where *a* and *r* indicate azimuthal angle and range, respectively. The variable *d* is the ground truth (with 1 and -1 represents convective and stratiform), i.e., the desired response in the training process.

7.) In section 3, the authors present the results of their work, introducing a whole coverage convective ratio (RCS) number. The latter is defined as parameter that provides a qualitative assessment of the performance of SVM and other considered methods. In my opinion, an evaluation about the reliability of SVM algorithm based on a single parameter is not sufficient to reach robust conclusions. Therefore, I suggest to involve in the statistical analysis other useful scores, such as the Critical Success Index and ROC curve.

Response: We agree with the reviewer that a single crietia may not sufficient to validate the performance of proposed approach. To address the reviewer's concerns, we made the following modifications:

1.) Besides the convective ratio (R^{CS}) we introduced in the original manuscript, we also applied the Probability of Detection (POD), False Alarm Ratio (FAR), and Critical Success Index (CSI) in the performance evaluation.

2.) Since both cases of 30 August 2011 and 14 June 2012 are widespread stratiform and convective mixed precipitation events, and the performances of proposed approach show similarity from these two cases. We only kept the 30 August 2011 cases in the revised manuscript for the stratiform and convective mixed precipitation case. We also added more analysis and sensitivity test on this case.

3.) For the tropical precipitation case 08/06/2009~08/09/2009 case, we included POD, FAR, CSI analysis, and also included sensitivity test.

Please refer section 3 in the revised manuscript for more details.

8.) Some suggestions about figures. In figure 1, I suggest to include a reference scale for terrain elevation.

Response: Following reviewer's suggestion, a reference scale for terrain elevation is added in the manuscript, as shown below.

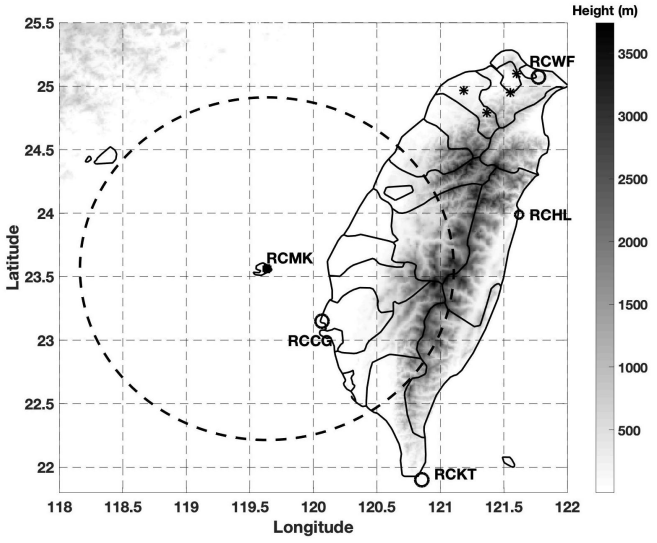

Figure 4. The terrain of Taiwan, the location of a C-band polarimetric radar RCMK (marked with a black square), JWDs (marked with black stars), and four S-band single polarization radar

RCCG, RCKT, RCHL, and RCWF (marked with black circles). The continuous grey-scale terrain map shows the central mountain range of Taiwan.

9.) In figure 3, it is necessary to improve the line-style used to indicate the various algorithm. More specifically, MRMS and SVM time series seem have a similar marker according to the legend showed in panel (a).

Response: Following reviewer's suggestion, we use different colors to represents the results from different algorithms. More details could be found from the response to comment 7.).

10.) Regarding figure 4, I recommend to enlarge the panels, if it is possible. Moreover, the color scale should not have a gradient, because the output of the algorithm is binary (convective or stratiform).

Response: Following reviewer's suggestion, we made following modifications: 1.) enlarge each panels in figure 4; and 2.) change the color scale as binary.

11.) About Figures 5, 6, and 7, please clarity in the caption the meaning of black, red, and white circles.

Response: Following reviewer's suggestion, we added the meaning of these circles in the caption.

12.) Finally, I suggest to carefully checking the paper to address some minor typos.

Response: Following reviewer's suggestion, we run grammar and spelling check before submitting the revision.

Reply to Referee 4

We appreciate the reviewer provided these important comments help us improving our manuscript. We'd like to address these comments as following.

1. ZDR is a moment that needs to be calibrated. How stable is the ZDR calibration with time for the C-band you are using. Usually one attempts to be within +/- 0.2 dB. Do you use birdbath scans to calibrate ZDR?

Response: Thank you for the reviewer pointing this out. We totally agree with the reviewer that calibration plays a critical role in radar data processing and weather radar applications. A bias within 0.2 dB is the basic requirement on the ZDR field. In the current work, we directly used the data provided by the radar engineers from Central Weather Bureau of Taiwan, and no further calibration was applied on the Z_{DR} field. We believed the quality of data is good, and the calibration bias of ZDR should be within the reasonable range based on following two reasons:

1.) This radar belongs to Weather Wing of the Chinese Air Force (CAF), and the data became available to the Central Weather Bureau (CWB) since 2009. Currently, RCMK is one of the operational radars in the radar network, and its data are used in the real-time quantitative precipitation estimation (QPE) and forecasting (QPF). The quality of the radar data is closely examined by the engineers from CAF and CWB. Therefore, we believe this radar is well maintained and calibrated.

2.) Same data sets (such as: 08/06/2009 ~ 08/09/2009) from this radar were also examined in few QPE papers (e.g., Wang et al. 2013, 2014). In order to achieve less than 10% bias in QPE products, the bias (including mis-calibration and attenuation) of reflectivity, and differential reflectivity should be within 1 dBZ, and 0.1 dB, respectively. Based on the QPE results estimated from this radar using different combinations of polarimetric radar variables, we believe the bias of Z and ZDR should be within a reasonable range.

On the other hand, following the reviewer's suggestion, we did the sensitivity analysis on the ZDR field. In this analysis, the observed ZDR field was manually adjusted by a factor of -0.2 dB, -0.1 dB, 0.1 dB, and 0.2 dB, respectively. The separation index was recalculated with the "biased" Z_{DR} field. The performances from proposed approach and using separation index only were analyzed with the "biased" fields. Please refer to the reply to comment 2 for more details related to this test.

2. How sensitive is the separation index (eq2) to a ZDR bias? You assume implicitly a perfect radar (hardware wise), where only attenuation corrections need to be applied (if necessary). I wonder how sensitive your method is to some radar hardware influences or issues. Or can you rule out any influence from radar hardware? A discussion is needed here.

Response: First, we do appreciate the reviewer pointing this out. We did not include sensitivity analysis in the original manuscript. We believe such analysis is very useful to guide readers to evaluate and apply this algorithm.

To address this concern, we did the sensitivity test through simulation and real data validation. In the simulation part, the separation index *i* was calculated with four distinct *Z* values: 10 dBZ, 20 dBZ, 30 dBZ, and 40 dBZ. For each *Z*, *ZDR* changes between -0.5 dB to 2 dB, which is used to simulate the bias on ZDR field. The simulation results could be found from revised manuscript in section 3.3.

In the real case validation, we did the following test:

1.) After correcting the Z_{DR} field from attenuation, we manually added ΔZ_{DR} values (as the designed bias) on the corrected Z_{DR} field. The ΔZ_{DR} values are: -0.2 dB, -0.1 dB, 0 dB, 0.1 dB, and 0.2 dB, and the "biased" Z_{DR}: are calculated as:

$$Z_{DR}^{b} = Z_{DR} + \Delta Z_{DR}$$

where Z_{DR}^{b} indicates biased Z_{DR}.

2.) Calculate the separation index (i^b) with Z_{DR}^{b}. Evaluate the impacts of ΔZ_{DR} on performances of BAL^0 and $BAL^{-0.5}$ on cases 08/30/2011 and typhoon case (08/06/2009~ 08/09/2009).

3.) With Z_{DR}^{b} and i^b as the inputs to the proposed SVM approach, Evaluate the impacts of ΔZ_{DR} on performances of SVM approach on cases 08/30/2011 and typhoon case (08/06/2009~ 08/09/2009).

More details about simulation and real data validation could be found in section 3.2 in the revised manuscript. In the revised manuscript, only the case from 08/30/2011 is provided. The results from 2009 are provided as below:

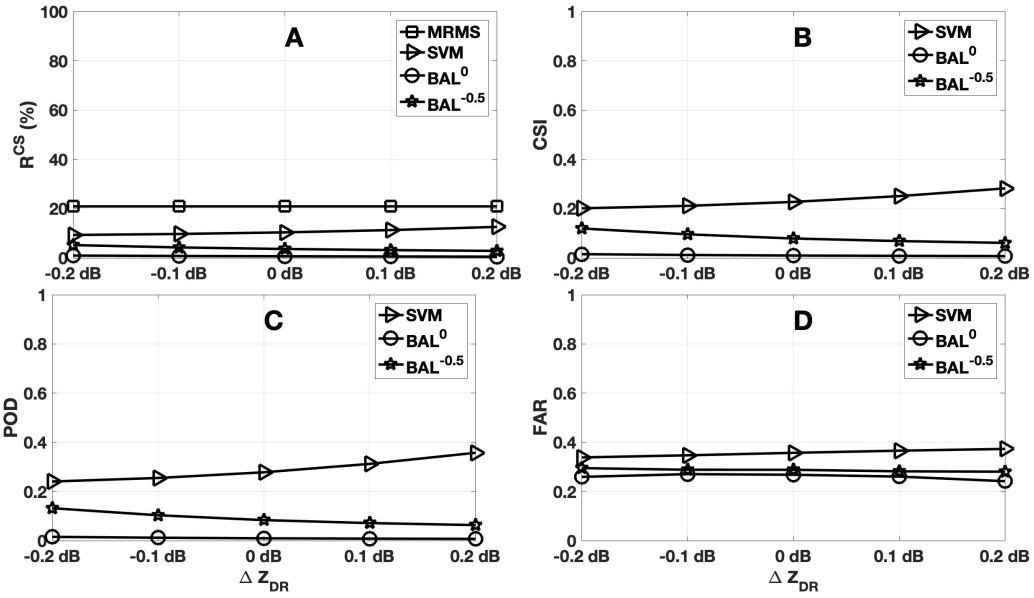

Figure 1. 96-hour averaged R^{CS}(A), CSI(B), POD(C), and FAR(D) from 6~9 August 2009. The results from BAL with threshold T_0 = -0.5, BAL with threshold T_0 = 0, SVM, and MRMS are indicated with symbols of pentagram, circle, triangle, and square, respectively.

Are the radome effects an issue (especially for the typhoon case you present; is it possible that part of the somewhat unusual ZDR pattern in Fig. 10 may be attributed to such a source?)

Response: Yes, we agree with the reviewer. The wet radome could be a possible issue for radar variables such as Z and Z_{DR}. In the revised manuscript, we added following discussion:

Line 280 Other reasons such as wet radome may also contribute to the Z and Z_{DR} issues.

L164, can you motivate why using such a large rhohv (> 0.98) as a criterion? You seem to throw away a lot of data e.g., if you have mixed phase precipitation with hail. Is there no hail in Taiwan? How much of the data are not considered? What happens if you observe rhohv < 0.98. How is the performance degrading if you have data ranges present that where considered for training. Those rangebins cannot be classified, since you trained the data for only specific ranges? Explain what consequence this choice of threshold has, how sensitive your results are, and before that, how the training results are dependent on this choice. Did you make sensitivity studies?

Response: We'd like to address the reviewer's concern from following few different aspects:

1.) In the manuscript, we use 0.98 as the threshold of RhoHV only in the training data selection. As reported by Kumjian (2013), pure rain generally produces very high of RhoHV (> 0.98) observed by WSR-88D. Such value (0.98) also suggested by Ryzhkov and Zrnic (2004) as the RhoHV field from majority of pure rain in C-band. Such large RhoHV was also suggested in hydrometeor classifications (e.g., Liu and Chandrasekar 2000; Park et al. 2009). For example, Park et al. (2009) suggested that RhoHVs for light/moderate rain, and heavy rain are 0.97 and 0.95, respectively. The precipitation may be classified as the mixed rain and hail if RhoHV is below 0.9. Following these pioneering works, we choose 0.98 as the threshold of RhoHV in the training data selection.

   In the revised manuscript, we added the reference paper on Line 186.

2.) The threshold of 0.98 for RhoHV is only applied in the training data selection. Such aggressive threshold can assure the training data from pure precipitation, and not smeared by clutter (including ground clutter, sea clutter, biological scatter), AP, and possible ice phase precipitation. When we test the algorithm with precipitation events, the threshold for RhoHV is selected as 0.90. Any pixel (gate) with RhoHV below than 0.9 is classified as non-precipitation echo. Any pixel with RhoHV above 0.9 is treated as pure rain, and the same support vector obtained from training data is applied.

3.) The separation index (i) was derived from two drop size distribution (DSD) parameters N_w and D_0. Therefore, it only validates at liquid phase precipitation (stratiform and convective types) as suggested by (Bringi et al. 2009). For other phase precipitation, such as mixed hail and rain, its performance is not well studied (Bringi et al. 2009). Other hydrometeor classification schemes are suggested for such scenario (Bringi et al. 2009). In this work, the separation index

also plays an important role in the SVM approach, therefore, we limited the application of the proposed approach only within pure water phase precipitation. We have not tested it on the mixed phase precipitation with hail. In the revised manuscript, we emphasized this limitation at Line 344.

4.) The goal of this work is to propose a prototype algorithm, and this manuscript focuses on describing this algorithm. We are working on further analyzing this approach including deriving the new separation index for S-band radar (WSR-88D), validating its long-term performance, including more variables (such as reflectivity texture), including multiple elevation angles. Sensitivity test for different training data definitely is also included in this work. We plan to report further findings in the upcoming papers.

L166, what is exactly a "data set"? A range bin with all the moments you use satisfying the criteria for Z, RhoHV? Would be helpful to the reader who is not so familiar with this method.

Response: We appreciate the reviewer pointing this out. A "set" means a set of data from one radar gate (defined as azimuthal angle and range). Be more specific, a set of training data means a vector of $[Z(a,r)\ Z_{DR}(a,r)\ i(a,r); d(a,r)]$. Where "*a*" indicates azimuthal angle, "*r*" indicates range; "d" is the desired response with "1" represents convective, and "-1" represents stratiform.

Line 188: A total of 17281 sets of data (15144 sets of stratiform, and 2137 sets of convective) are used in the training process. In this work, one data set is defined as the variables from a single gate in terms of range and azimuthal angle. Be more specific, a collection of training data means a vector of [$Z(a, r)$ $Z_{DR}(a, r)$ $i(a, r)$ $d(a, r)$], where *a* and *r* indicate azimuthal angle and range, respectively. The variable *d* is the ground truth (with 1 and -1 represents convective and stratiform), i.e., the desired response in the training process.

L234: the intrinsic ZDR for stratiform precipitation: isn't it something around 0.2 dB, Or is this different in Taiwan?

Response: Yes, the reviewer is correct. The ZDR values we provided in the manuscript is not accurate. The ZDR values mentioned in the manuscript are within the black circle in the following figure (Fig. 7 in the original manuscript). If we examine carefully, especially for those gates with Z around 30 dBZ, the ZDR values are around 0.2 dB, instead of 0 dB.

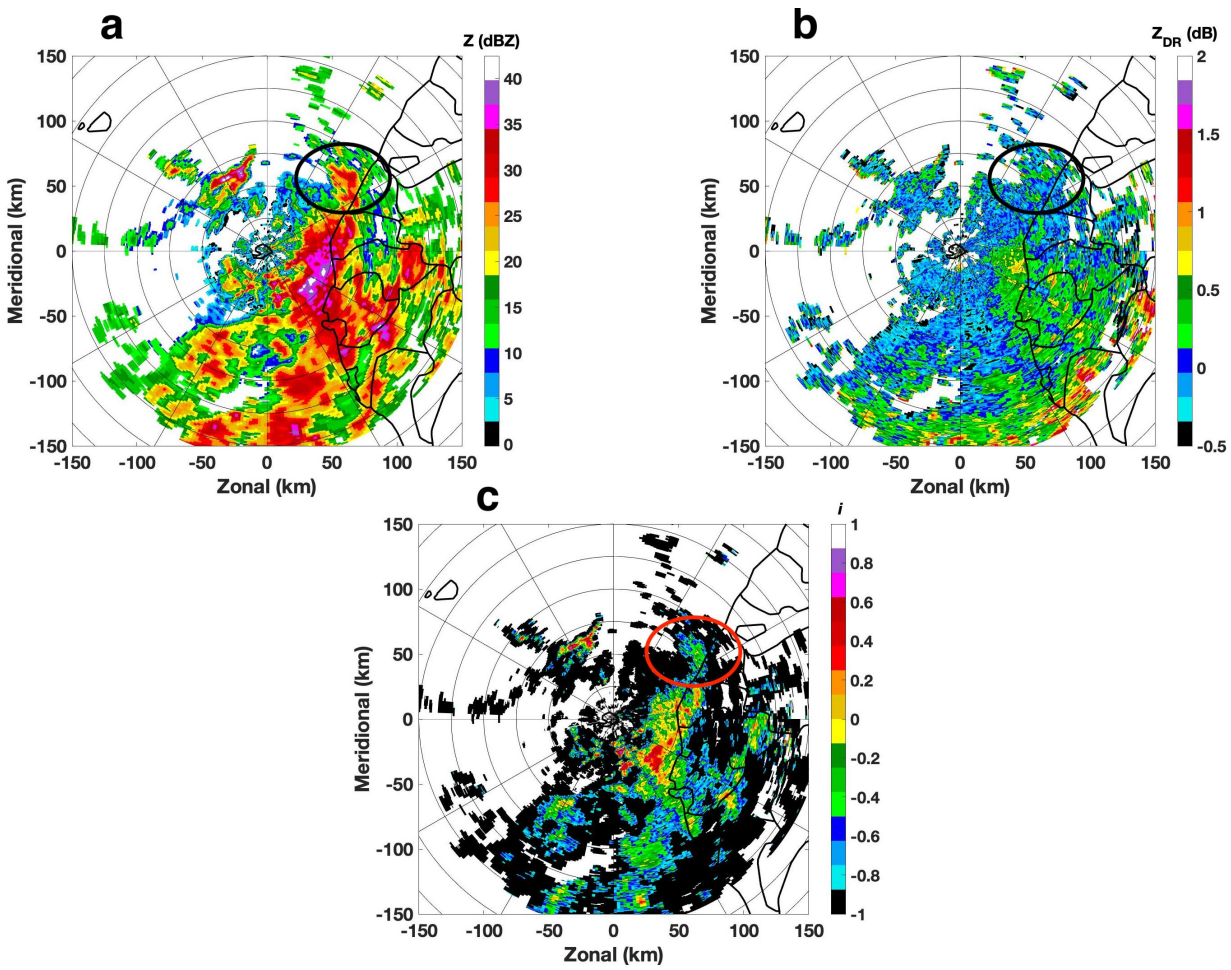

Fig 10: ZDR looks biased to me… There seem sector based (az, range) biases for 270 -> 90°… you mention this in I250 ff, but Z looks relatively reasonable here.

Response: We agree with the reviewer. In this sector, ZDR looks over corrected from attenuation, but Z looks relatively better. One hypothesis is both coefficients α and β used in the linear PhiDP are need be adjusted based on the DSD and DSR features. Comparing to α, β is more sensitive to the impact of DSD and DSR.

Reference:

Kumjian, M. R., 2013: Principles and applications of dual-polarization weather radar. Part I: Description of the polarimetric radar variables. *J. Operational Meteor.,* **1** (19), 226-242, doi: http://dx.doi.org/10.15191/nwajom.2013.0119.

Liu, H., and V. Chandrasekar, 2000: Classification of hydrometeors based on polarimetric radar measurements: Development of fuzzy logic and neuro-fuzzy systems, and in situ verification. *J. Atmos. Oceanic. Technol*., **17**, 140-164.

Park, H, A. V. Ryzhkov, D. S. Zrnic, and K.-E. Kim, 2009: The hydrometeor classification algorithm for the polarimetric WSR-88D: description and application to an MCS. *Weather and Forecasting*, **24**, 730-748.

Ryzhkov A. and D. Zrnic, 2004: Radar polarimetry at S, C, and X bands: comparative analysis and operational implications. *32nd Conference on Radar Meteorology*. 9R.3 24~29 May 2004

Wang, Y., P. Zhang, A. V. Ryzhkov, J. Zhang, and P.-L. Zhang 2014: Utilization of specific attenuation for tropical rainfall estimation in complex terrain. *Journal of Hydrometeorology*, vol 15, 2250-2266.

Wang, Y., J. Zhang, A. Ryzhkov, and L. Tang, 2013: C-band polarimetric radar QPEs based on specific differential propagation phase for extreme typhoon rainfall*. J. Atmos. Oceanic Technol*., vol 30, 1354-1370..

Separation of Convective and Stratiform Precipitation Using Polarimetric Radar Data with A Support Vector Machine Method

Yadong Wang[1], Lin Tang[2], Pao-Liang Chang[3], and Yu-Shuang Tang[3]

[1]Electrical and Computer Engineering Department, Southern Illinois University Edwardsville, Illinois, USA
[2]Cooperative Institute for Mesoscale Meteorological Studies, University of Oklahoma, NOAA/OAR/National Severe Storms Laboratory, Norman, Oklahoma, USA
[3]Central Weather Bureau, Taipei, Taiwan

Correspondence: Yadong Wang (yadwang@siue.edu)

Abstract. A precipitation separation approach using a support vector machine method was developed and tested on a C-band polarimetric weather radar located in Taiwan (RCMK). Different from some existing ~~separation methods that require~~ methods requiring a whole volume ~~radar~~ scan data, the proposed approach utilizes the polarimetric radar data from the lowest unblocked tilt to classify precipitation echoes into either stratiform or convective type. ~~Through a support vector machine method, the~~ The inputs of radar reflectivity, differential reflectivity, and the separation index are ~~utilized in the classification~~ integrated into the classification through a support vector machine algorithm. The feature vector and weight vector in the support vector machine were optimized using well-classified training data. The proposed approach was tested with multiple precipitation events including ~~two widespread mixture of~~ a widespread mixed stratiform and convective ~~events~~event, a tropical typhoon precipitation event, and a stratiform precipitation event. In the evaluation, the results from the multi-radar-multi-sensor (MRMS) precipitation classification ~~approach~~ algorithm were used as the ground truth~~, and the performances from~~. The performances from the proposed approach were further compared with the approach using the separation index only~~with different thresholds~~. It was found that the proposed method can accurately ~~identify the convective cells from stratiform storms with the radar data only from the lowest scanning tilt. It can~~ classify the convective and stratiform precipitation, and produce better results than using the separation index only.

1 Introduction

Convective and stratiform ~~precipitation systems exhibit significant differences~~ precipitations exhibit a significant difference in precipitation growth mechanisms and thermodynamic structures (e.g., Houghton, 1968; Houze, 1993, 1997). Generally, ~~convective precipitations are~~ a convective precipitation is associated with strong ~~and~~ but small areal vertical air motion (> 5 m s^{-1}) ~~, while stratiform precipitations are associated with weak and mesoscale updrafts/downdrafts (< 3 m s^{-1}) (Penide et al., 2013). Moreover, a convective system consists of large and dense raindrops generally delivers~~ (Penide et al., 2013), and delivers a high rainfall rate (R) ~~; a stratiform precipitation, on~~ (Anagnostou, 2004). On the other hand, stratiform precipitation is associated with ~~relative~~ weak updrafts/downdrafts (< 3 m s^{-1}) and relatively low R~~(Anagnostou, 2004). Accurately separating convective type from stratiform precipitations~~. Classifying a precipitation into either convective or

stratiform type not only promotes the understanding of cloud physics but also enhances the accuracy of quantitative precipitation estimation (QPE). ~~Numerous precipitation classification algorithms~~ For these purposes, numerous methods using ground in situ measurements or satellite observations were developed during the past four decades (e.g., Leary and Jr., 1979; Adler and Negri, 1988; Tokay and Short, 1996; Hong et al., 1999).

Ground-based weather radars, such as Weather Surveillance Radar, 1988, Doppler (WSR-88D), are currently used in ~~severe weather detection, hydrometeor classification, QPE, and other meteorological applications~~all aspects of weather diagnosis and analysis. Precipitation classification ~~methods were developed~~ algorithms using single- or dual-polarization radars were developed during the past three decades. For a single-polarization radar, developed ~~classification~~ algorithms mainly rely on radar reflectivity (Z) and its derived variables ~~(e.g., Steiner et al., 1995), (hereafter SHY95) (Biggerstaff and Listemaa, 2000; Anagnostou,~~ (e.g., Biggerstaff and Listemaa, 2000; Anagnostou, 2004; Yang et al., 2013; Powell et al., 2016). For example, ~~based on the study from Steiner and Houze (1993),~~ Steiner et al. (1995) (hereafter SHY95) proposed a separation approach that utilizes the texture features derived from the radar reflectivity field. In this approach, a grid point in the Z field is identified as the convective center if its value is larger than 40 dBZ, or exceeds the average intensity taken over the surrounding background by specified thresholds. Those grid points surrounding the convective centers are classified as convective area, and far regions are classified as stratiform. ~~During their experiments,~~ Penide et al. (2013) found that SHY95 ~~misclassified~~ may misclassify those isolated points embedded within stratiform precipitation or associated with low cloud-top height. Powell et al. (2016) modified the SHY95′s approach, and the new approach can identify shallow convection embedded within large stratiform regions~~, and those isolated shallow and weak convections~~. A neural network based convective-stratiform classification algorithm was developed by Anagnostou (2004). ~~It utilizes six variables~~ Six variables were used in this approach as inputs including storm height, reflectivity at 2 km elevation, the vertical gradient of reflectivity, the difference in height, the standard deviation of reflectivity, and the product of reflectivity and height. Similar variables ~~are~~ were also used in ~~the~~ a fuzzy logic based classification approach proposed by Yang et al. (2013). ~~In these two approaches, a full volume of radar reflectivity field is needed to calculate variables such as the product of rain column top height reflectivity value at 2 km, and the vertically integrated liquid water content.~~

~~According to~~

Although these listed classification algorithms have been developed and validated for years, a new robust algorithm is motivated for the following two reasons. The first is to utilize only the low tilt radar data for classification. According to the U.S. Radar Operations Center (ROC), the WSR-88D radars are currently operated without updating a complete volume during each volume scan, especially during precipitation events. New radar scanning schemes are designed to reorganize the updating order for a high frequency in low elevations and a less frequency for high elevations. ~~Therefore,~~ An alternative scanning scheme enables the WSR-88D radars are able to promptly capture the storm development for weather forecast and to obtain a more accurate precipitation estimation. These new schemes include the automated volume scan evaluation and termination (AVSET), supplemental adaptive intra-volume low-level scan (SAILS), the multiple elevation scan option for SAILS, and the mid-volume rescan of low-level elevations (MRLE). Under these new scanning schemes, the separation of stratiform/convective becomes a challenge for those algorithms ~~require~~ requiring a full volume ~~of radar data.~~

~~Polarimetric radars transmit and receive electromagnetic waves along the horizontal and vertical directions, and therefore can obtain extra information about hydrometers~~ scan of data. The second reason is to further explore the applications of the polarimetric variables. Polarimetric weather radars have been well applied in radar QPE, severe weather detection, hydrometeor classification, and microphysical retrievals (Ryzhkov and Zrnic, 2019; Zhang, 2016). Extra information about hydrometeors' size, shape, species, and orientation ~~. A~~ could be extracted through transmitting and receiving electromagnetic waves along the horizontal and vertical directions. Therefore, the polarimetric measurements may reveal more precipitation's microphysical and dynamic properties. Inspired by these features, a C-band polarimetric radar precipitation separation approach was developed by Bringi et al. (2009) (hereafter BAL), which classifies the precipitation into stratiform, convective and transition regions based on retrieved drop size distribution (DSD) characteristics. ~~However, the performance of DSD-based approach depends on the environment regime (Thompson et al., 2015). Strong~~ However, it was found that strong stratiform echoes might have similar DSDs to weak convective echoes and lead to wrong classification results (Powell et al., 2016).

In this work, a novel precipitation separation algorithm using the separation index with other radar variables was developed and tested on a C-band polarimetric radar located in Taiwan. This approach classifies precipitations into stratiform or convective ~~types using~~ type with a support vector machine (SVM) method. Different from some existing classification techniques that ~~utilize the whole volume~~ require a whole volume scan of radar data, this new approach uses the ~~unblocked data from the lowest scanning tilt . The C-band polarimetric radar~~ lowest unblocked tilt data in the separation. If the lowest tilt is partially or completely blocked, then the next adjacent unblocked tilt is used instead. The major advantage of this method is that it can provide real-time classification results even ~~it~~ if the radar is operated under AVSET, SAILS, and MRLE scanning schemes, where the ~~lowest tilt is the most~~ low tilts are frequently scanned and updated. ~~All the parameters used in the current approach are trained from typical convective and stratiform precipitation events.~~ This paper is organized as follows: Section 2 introduces the ~~radar features and the radar data processing; Section 3 proposes the classification using support vector machine;~~ proposed method including radar variables and processings, the SVM method, and the training process. The performance evaluation is shown in Section ~~4, and a~~ 3, and the discussion and summary are given in Section ~~5.~~ 4.

2 ~~Methodology~~Precipitation Separation With a Support Vector Machine Method

2.1 ~~Radars and Joss-Waldvogel Disdrometers~~

In the current work, the SVM precipitation ~~classification~~ separation approach was developed and validated on a C-band polarimetric radar (RCMK) located at Makung, Taiwan (Figure 1). The Weather Wing of the Chinese Air Force deployed this radar and made the data available to the Central Weather Bureau (CWB) of Taiwan since 2009. Together with ~~other~~ three single-polarization S-band WSR-88D (RCCG, RCKT, and RCHL) and one dual-polarization S-band radar (RCWF), these five radars provide real-time ~~QPEs for~~ QPE products to CWB to support missions of flood monitoring and prediction, landslide forecasts and water resource management. Operating with a wavelength of 5.291 cm, RCMK performs volume scans of 10 tilts (0.5°, 1.4°, 2.4°, 3.4°, 4.3°, 6.0°, 9.9°, 14.6°, 19.5°, and 25°) in every 5 minutes with the range resolution of 500 m and angular sampling of 1°.

~~In order to understand DSD features in Taiwan from convective and stratiform precipitations, total 4306 minutes DSD data between 2011 to 2014 were used in the analysis as shown in section 2.2. The DSD data were collected by four impact-type Joss-Waldvogel disdrometers (JWD) , and the locations of these four JWDs are shown in Figure 1. The measurement range and temporal resolution of these JWDs are 0.359 mm ~ 5.373 mm and 1 minute, respectively~~The Central Mountain Range (CMR) of Taiwan is also shown in Figure1, which poses a major challenge for radar based products. Radars located in complex terrain are prone to partial or total blockages, which cause data from the low elevation angles (EA) to be unavailable or problematic. Blockage maps of RCMK are illustrated in Figure 2. Since there are severe blockages at the 0.5° for RCMK, data from the 1.4° EA is used in the algorithm development.

2.1 Input ~~Polarimetric Radar Variables~~ polarimetric radar variables and ~~Preprocess~~preprocesses

~~The inputs of~~ Three measured or derived radar variables are proposed as inputs to the SVM approach~~are three variables~~: Z, differential reflectivity fields (Z_{DR}), and separation index (i). In most of ~~the~~ precipitation classification approaches, Z is used as ~~the input because reflectivities from convective systems~~ one of the inputs because reflectivity from convective generally show higher values than from stratiform ~~systems. In the approach developed by SHY95~~type. For example, a radar echo, with the reflectivity of 40 dBZ and above, is automatically classified as convective type ~~. Stratiform precipitations generally consist of condense of small to median raindrops, which generally produce a low value of Z_{DR}. The convective precipitation , on the other hand, may produce large~~ in the approach developed by SHY95.

Differential reflectivity, which is highly related to raindrop's mass weighted mean diameter (D_m), is another good indicator of precipitation type. It was found the values of D_m in stratiform and convective precipitation generally are within 1-1.9 mm and above 1.9 mm, respectively (Chang et al., 2009). Higher Z_{DR} ~~because they consist of large and oblate raindrops~~values are expected from convective than from stratiform precipitation. Therefore, the Z_{DR} field is used as another input of the proposed approach.

For short wavelength radars such as C-band or X-band radars, the Z and Z_{DR} fields may be ~~significant attenuated when the~~ significantly attenuated when radar beam propagates through heavy precipitation regions. Both Z and Z_{DR} fields need to be corrected from attenuation before applied in the precipitation classification and QPE. Different attenuation correction methods were proposed using the differential phase (ϕ_{DP}) measurement such as ~~linearly approach,~~ the linear ϕ_{DP} approach, the standard ZPHI method, and the iterative ZPHI method (e.g., Jameson, 1992; Carey et al., 2000; Testud et al., 2000; Park et al., 2005). Because of its simplicity and easy implementation in a real-time system, the linear ϕ_{DP} method was applied in the current work.

$$Z(r) = Z'(r) + \alpha(\phi_{DP}(r) - \phi_{DP}(0)) \tag{1a}$$

$$Z_{DR}(r) = Z'_{DR}(r) + \beta(\phi_{DP}(r) - \phi_{DP}(0)) \tag{1b}$$

where $Z'(r)$ ($Z'_{DR}(r)$) is the observed reflectivity (differential reflectivity) at range r; $Z(r)$ ($Z_{DR}(r)$) is the corrected value; $\phi_{DP}(0)$ is the system value; $\phi_{DP}(r)$ is the smoothed (by FIR filter) differential phase at range r. The attenuation correction coefficients α and β depend on DSD, drop size shape relations (DSR), and temperature. The typical range of α (β) is found

0.06∼0.15 (0.01∼0.03) dB deg^{-1} for C-band radars (e.g., Carey et al., 2000; Vulpiani et al., 2012). Following the work from Wang et al. (2014), optimal coefficients α and β in Taiwan are 0.088 dB deg^{-1} and 0.02 dB deg^{-1}, respectively. The Z and Z_{DR} fields are further smoothed with a 3 (azimuthal) by 3 (range) moving window function after corrected from attenuation.

Other quality control issues, including calibration, reflectivity vertical profile, and ground clutter removal, were also considered in this work. Since this radar is used in the real-time quantitative precipitation estimation, the biases of Z and Z_{DR} should be within 1 dBZ, and 0.1 dB, respectively. The data quality of RCMK was examined through validating the QPE performance in different works (e.g., Wang et al., 2013, 2014). Therefore, the calibration bias of RCMK should be within the reasonable range. A vertical profile of reflectivity (VPR) correction is generally needed on the reflectivity field to reduce the measurement biases because of the melting layer (Zhang et al., 2011). Given the fact that 1.4° elevation angle is used within the maximum range of 150 km, and the melting layer is usually around 5 km in Taiwan, the radar data is well below the melting layer. In addition, considering the vertical profile of differential reflectivity is not well studied in the current stage, no vertical corrections are applied to fields of Z and Z_{DR}. Ground clutter is typically associated with a low correlation coefficient (ρ_{HV}), the ρ_{HV} threshold used in this work is 0.9, which can effectively remove those non-meteorological echoes such as ground clutter.

Using the separation index i to identify convective ~~precipitation from stratiform was proposed initially by BAL using a C-band polarimetric radar. According to BAL,~~ from stratiform precipitation was initially proposed by BAL, where i was calculated under a normalized gamma DSD assumption:

$$i = log_{10}(N_W^{est}) - log_{10}(N_W^{sep}) \tag{2}$$

$$log_{10}(N_W^{sep}) = -1.6D_0 + 6.3 \tag{3}$$

where N_W^{est} is the estimated N_W (normalized number concentration) from observed Z and Z_{DR}, and is calculated as:

$$N_W^{est} = Z/0.056D_0^{7.319} \tag{4}$$

In Equation 4, D_0 is the median volume diameter ~~D_0 is~~ and can be calculated as.

~~$D_0 = 0.0203Z_{DR}^4 - 0.1488Z_{DR}^3 + 0.2209Z_{DR}^2 + 0.5571Z_{DR} + 0.801; \ -0.5 \le Z_{DR} < 1.25$~~

~~$= -0.0355Z_{DR}^3 - 0.3021Z_{DR}^2 + 1.0556Z_{DR} + 0.6844; \ 1.25 \le Z_{DR} < 5$~~

$$D_0 = 0.0203Z_{DR}^4 - 0.1488Z_{DR}^3 + 0.2209Z_{DR}^2 + 0.5571Z_{DR} + 0.801; \ -0.5 \le Z_{DR} < 1.25 \tag{5a}$$

$$= -0.0355Z_{DR}^3 - 0.3021Z_{DR}^2 + 1.0556Z_{DR} + 0.6844; \ 1.25 \le Z_{DR} < 5 \tag{5b}$$

The units of Z_{DR}, Z, N_w, and D_0 are dB, mm^{6}m^{-3}, mm^{-1}m^{-3}, and mm, respectively. The positive and negative values of index i indicate convective and stratiform rain, respectively, and $|i| < 0.1$ indicates transition regions (Penide et al., 2013). BAL pointed out that index i worked well in most of the cases in their study; however, incorrect classification results are likely obtained for low Z and high Z_{DR} cases in some convective precipitations.

2.2 Drop size distribution and drop shape relation

It should be noted that the relations between ~~Z~~i, N_w, and D_0 were derived using the DSD data collected in Darwin, Australia. Coefficients in Equations 2∼5 need be adjusted according to ~~different frequency radars~~ the radar frequency or/and ~~other~~ DSD and DSR features from the specific location (Thompson et al., 2015). In the current work, the separation index i is directly derived using Equations 2∼5 ~~is directly used as one of the input variables~~without further adjustment. It was shown by Wang et al. (2013) that DSD and DSR features in Taiwan ~~is~~ are very similar to those measured from Darwin, Australia. Similar $R(K_{DP})$ relationships were obtained using data collected from these two locations. Coefficients derived by BAL could be directly used in Taiwan without further modification. To verify this assumption, N_w and D_0 were calculated using DSD data collected by four ~~JWDs~~ impact-type Joss-Waldvogel disdrometers (JWD) located in Taiwan (Figure 1). ~~Total~~ The measurement range and temporal resolution of these JWDs are 0.359 mm ∼ 5.373 mm and 1 minute, respectively. A total of 4306-minute data from 2011∼2014 are used in N_w and D_0 calculation following the approach described in Bringi et al. (2003). Similar to the work presented in BAL, the distribution of i along median volume diameter D_0 is shown in Figure 2, where ~~the~~ ($log_{10}N_w$, D_0) pairs from stratiform and convective types are represented with gray circles and black stars, respectively. Although the relation described in Equation 3 can separate most stratiform from convective ~~types~~type, a large number of points are still classified incorrectly. Therefore, the single separation index is not sufficient in the precipitation separation, and other variables such as Z and Z_{DR} may be used as ~~the supplement~~supplements.

3 ~~Support Vector Machines (SVM) Method~~

2.1 ~~Introduction of~~ Support vector machines (SVM) method

2.1.1 Introduction of SVM

Machine learning algorithms based on meteorological radar data were well developed during the past two decades (e.g., Capozzi et al., 2018). Support vector machine (SVM) can be viewed as a kernel-based machine learning approach, which nonlinearly maps the data from the low-dimension input space to a high-dimension feature space, and then linearly maps to a binary output space (Burges, 1998). Given a set of training samples, the SVM constructs an optimal hyperplane, which maximizes the margin of separation between positive and negative examples (Haykin, 2011). Specifically, given a set of training data $\{(X_i, y_i)\}_{i=1}^{N}$, the goal is to find the optimal weights vector W and a bias b such that

$$y_i(W^T X_i + b) \geq 1 \qquad i = 1, 2, ..., N \tag{6}$$

where $X_i \in \mathbb{R}^m$ is the input vector, m is the ~~input~~ variable dimension (m = 3 in this work), N is the number of training samples, and y_i is ~~an~~ the output with the value of $+1$ or -1 that represents convective or stratiform, respectively. The particular data points (X_i, y_i) are called support vector when Equation 6 is satisfied with the equality sign. The optimum weights vector W and bias b can be obtained through solving the Lagrangian function with the minimum cost function (Haykin, 2011).

Since the SVM can be viewed as a kernel machine, finding the optimal weight vector and bias in Equation 6 can be alternatively solved through the recursive least square estimations of:

$$\sum_{i=1}^{N_s} \alpha_i y_i k(X, X_i) = 0 \tag{7}$$

where N_s is the number of support vectors, α_i is the Lagrange multipliers, and $k(X, X_i)$ is the Mercer kernel defined as:

$$k(X, X_i) = \Phi^T(X_i)\Phi(X) = exp\left(-\frac{1}{2\sigma^2}||X - X_i||^2\right) \tag{8}$$

With the solved $\{\alpha_i\}_{i=1}^{N}$, the SVM calculate the classification results with new input data $Z \in \mathbb{R}^m$ as:

$$f(Z) = sign[\left[\sum_{i=1}^{N_s} \alpha_i y_i \Phi^T(X_i)\Phi(Z)\right] \tag{9}$$

When $f(Z) = 1$, the output is classified as convective, otherwise is classified as stratiform.

2.2 ~~Training of the SVM~~

2.1.1 Training of the SVM

In the SVM approach, the weight vector and bias in Equation 6 need to be optimized through a recursive least square estimation using ~~the training dataset~~training data. Since the training data play a critical role in the SVM approach, Z, Z_{DR} and i from convective and stratiform precipitation events were carefully examined through three steps. Firstly, the training data ~~is checked following some~~ was checked following general classification principles. For example, training data from convective precipitation is generally associated with ~~relative strong reflectivity , no apparent bight band signature,~~ relatively strong reflectivity and high vertically integrated liquid (VIL). ~~The precipitation type is then~~ On the other hand, stratiform precipitations are generally associated with a prominent bright band signature. The melting hydrometeors within the bright band increase backscatter during stratiform rainfall, which can significantly enhance radar reflectivity. The bright band feature is one of the obvious indicators of stratiform precipitation. Bright band signature normally can be observed from relatively high EAs (such as above 9.9°). From low EAs, because of the combination of radar beam broadening and low slant angle, the bright band feature spreads into more gates and becomes not apparent. Therefore, in this work, the bright band feature from high elevation angles is only used in training data selection but not used as one of the inputs. Secondly, the precipitation type is verified by ground observation~~such as gauge measurements and~~ , such as ground severe storm ~~observations. The precipitation types were finally~~ reports. Thirdly, the precipitation type is confirmed by the Multi-Radar-Multi-Sensor (MRMS) precipitation classification algorithm implemented in Taiwan (Zhang et al., 2011, 2016). In this MRMS classification approach, a ~~3-dimensional~~ three-dimensional radar reflectivity field was mosaicked from 4 S-band ~~single polarization~~ single-polarization radars (Figure 1), ~~and the~~ The composite reflectivity (CREF) ~~together with other fields~~ and other measurements such as temperature and moisture fields were then used in the surface precipitation classification (Zhang et al., 2016). ~~Seven different categories of warm stratiform, cold stratiform, convective, tropical stratiform, tropical convective, hail and snow are outputs of the MRMS precipitations~~

~~classification algorithm (Zhang et al., 2016).~~ Based on the classification results, MRMS ~~utilizes~~ chooses different $R(Z)$ relations in the rainfall rate estimation. The performance of MRMS has been thoroughly evaluated for years for the quantitative precipitation estimation, flash flood monitoring, severe weather, and aviation weather surveillance (e.g., Gourley et al., 2016; Smith et al., 2016)~~, and also~~ . The products are used as the benchmark and/or ground truth in many studies (e.g., Grecu et al., 2016; Skofronick-Jackson and Coauthors, 2017). ~~Therefore, the MRMS precipitation classification results were used as the ground truth~~ It should be noted that, on the other hand, the MRMS also shows limitations since it only uses single-polarization variables to determine the precipitation type. At the current stage, the MRMS precipitation classification is considered as the appropriate benchmark in the training and validation of the proposed algorithm. Moreover, since the MRMS classification ~~results are~~ is a mosaicked product derived from 4 S-band radars, it can be viewed as an independent reference.

~~Training data for convective type are~~ Convective type training data is mainly from a strong convective precipitation event on 23 July 2014. This thunderstorm, classified as convective precipitation by MRMS, was associated with strong updrafts/downdrafts and caused an aircraft crash on the airport of Makung at 1106 UTC. ~~Total 1-hour data~~ The squall line features can be clearly identified from this storm. Radar data collected from 1030 to 1130 UTC were used as the convective type training data~~, and the training data are associated with~~ . The training data selection follows the criteria of $Z > 20$ dBZ, and correlation coefficient $(\rho_{HV}) > 0.98$ (Kumjian, 2013). The stratiform type data are from a ~~mixture of stratiform /convective precipitation even~~ mixed stratiform and convective precipitation event on 30 August 2011, and only those data identified as a stratiform type by MRMS are used in training. ~~Total~~ A total of 17281 sets of data (15144 sets of stratiform, and 2137 sets of convective) are used in the training process. ~~The~~ In this work, one data set is defined as the variables from a gate in terms of range and azimuthal angle. Be more specific, a set of training data means a vector of $[Z(a,r)\ Z_{DR}(a,r)\ i(a,r)\ d(a,r)]$, where a and r indicate azimuthal angle and range, respectively. The variable d is the ground truth (with 1 and -1 represents convective and stratiform), which is as the desired response in the training process. The number of support vectors is selected as 1000 in the current work, and the training process is considered as completed when the root-mean-square error reaches a stable value. ~~It should be noted that with more support vectors, the SVM algorithm should have better performance but with higher computationcost~~In the SVM approach, the original three-dimension input space nonlinearly maps to a 1000-dimension feature space, and then linearly maps to a binary output space (Burges, 1998). The higher dimension feature space potentially captures more input variables features with higher computation cost. Generally, after the number of support vector reaches some number, the enhancement in the SVM's performance approach becomes slight. There is a balance between accuracy and computation. In the current work, the ~~numbers~~ number of support vectors ~~were tested at~~ was tested with a value of 500, 750, 1000, 2000, and ~~5000, and~~ 5000. The testing of 1000 support vectors can produce less than 5% error with reasonable computation time. As the prototype algorithm, the number of support vectors is selected as 1000 in the current work.

3 Performance Evaluation

3.1 Description of the experiments

The performance of the proposed approach was validated with ~~four~~ three precipitation events from 2009 to ~~2012. These four~~ 2011. These three precipitation events include one stratiform ~~event, one strong tropical precipitationevent, and two events of the mixture of~~ precipitation, one intense tropical precipitation, and one mixed convective and stratiform precipitation. Two experiments based on the BAL approach with different thresholds (i.e., BAL^0 and $BAL^{-0.5}$) were also carried out in the evaluation. In these two experiments, the separation index i from each radar gate is first calculated using Equations 2∼5, and thresholds of T_0 = 0 and -0.5 are then used to separate convective type from stratiform type. A ~~pixel~~ gate is classified as convective if i is larger than T_0, and as stratiform otherwise. This work aims ~~at developing~~ to develop a complementary method using separation index i ~~together with~~ and other variables to separate convective from stratiform type. The proposed SVM and BAL methods ~~both~~ can classify the precipitation using the lowest tilt radar data only, which is suitable for fast scanning and ~~quick updated purpose~~quickly updated purposes. Other classification approaches as introduced in section 1 were not examined in the current work, because they require the data from multiple elevation angles.

~~The MRMS classification products~~ In the evaluation, three statistical scores of probability of detection (POD), false alarm rate (FAR), and critical success index (CSI) are first used, and MRMS classification results are used as the ~~reference~~ "ground truth" in the ~~evaluation. Because the MRMS~~ calculation.

$$POD = \frac{hit}{hit + miss} \tag{10}$$

$$FAR = \frac{false}{hit + false} \tag{11}$$

$$CSI = \frac{hit}{hit + false + miss} \tag{12}$$

where "hit," "false," and "miss" are defined as a radar gate classified as convective type by MRMS and the evaluated approach simultaneously, by the evaluated approach only, and by MRMS only, respectively. Although these scores are well used in statistical analysis, two factors make it necessary to introduce one more criterion in the evaluation. First, MRMS results are derived using the mosaicked field from four S-band single-polarization radars, ~~the coverage and time stamp are different from the result of the single radar RCMK . The classification~~ and the classification results are produced every 10 minutes. On the other hand, BAL^0 , $BAL^{-0.5}$, and SVM generate classification results whenever RCMK completes a whole scan. The time difference between results from RCMK (~~i.e.,~~ BAL^0 , $BAL^{-0.5}$, and SVM) and MRMS could be ~~different~~ as large as 5 minutes~~in time stamps. Given the fact that the convective storms~~ . Second, a convective storm's size, intensity, and cells locations could change significantly during a ~~5-minute period, it is not feasible to evaluate the performance using the~~ short period. Therefore,

these three pixel-to-pixel ~~evaluation criteria of the possibility of detection (POD) and false alarm rate (FAR). We introduce a~~ based evaluation scores cannot really reflect the performance of the proposed approach. As a supplement, a whole coverage convective ratio (R^{CS}) ~~to evaluate the performance qualitatively:~~ is introduced in the current work:

$$R^{CS} = \frac{N^{con}}{N^{con} + Nstr} \frac{N^{con}}{N^{con} + N^{str}} \times 100\% \quad (13)$$

Where N^{con} and N^{str} are the total pixel numbers of convective and stratiform types within the coverage, respectively. Together with CSI, POD and FAR, these four scores are used in the performance qualitative validation. The evaluation results are shown in the following sections~~, and the overall performances of R^{CS} from the evaluation cases are presented in Table 1.~~ .

3.2 ~~Experiment results~~

3.2 Experiment results

3.2.1 Widespread ~~Mixtures of Stratiform~~ mixed stratiform and ~~Convective~~convective precipitations

The performance of the proposed approach was first validated with ~~two widespread mixture of~~ one widespread stratiform and convective ~~precipitation events from~~ mixed precipitation event on 30 August 2011, and ~~14 June 2012. For these two cases,~~ 24-hour data (0000 UTC∼2400 UTC) were used in the evaluation. ~~The~~ Classification results from the proposed SVM were calculated with the trained weight vector and biases, and results from the BAL approach (BAL^0 and $BAL^{-0.5}$) were also calculated for the comparison purpose. It should be noted that the threshold of -0.5 is much lower than the value suggested by BAL, and ~~more pixels will be classified as convective by $BAL^{-0.5}$. The classification results from the proposed SVM were calculated using the trained weight vector and biases, and the convective ratios from MRMS, SVM,~~ BAL^0~~, and $BAL^{-0.5}$ were calculated using Equation 10.~~

~~The time series plots of RCS are~~ may classify more precipitations as convective type.

The time series of R^{CS} (A), CSI (B), FOD (C), and FAR (D) are calculated using Equations 10∼13 and shown in Figure ~~3~~4, where results from ~~30 August 2011 and 14 June 2012 are shown on panel "a" and "b", and the RCS from~~ MRMS, SVM, BAL^0, and $BAL^{-0.5}$ are presented by ~~thick solid, thick dashed, thin solid and thin dashed~~ black, red, blue, and green lines, respectively. ~~In general, BAL~~When the MRMS results are applied as the ground truth, BAL^0 obviously classifies more precipitation as stratiform type during this 24-hour period. The time series of R^{CS} from BAL^0 are much lower than other three approaches. $BAL^{-0.5}$ classifies more pixels as convective than BAL^0 as expected~~for both cases, and~~ , and the R^{CS} scores are much higher than BAL^0. The proposed SVM shows the most similar ~~results~~ R^{CS} scores to MRMS comparing to BAL approaches. ~~For the 30 August 2011 case (Figure 3a), if the MRMS results are considered as the ground truth, BAL^0 shows obvious under classification of convective type during this 24-hour period, but $BAL^{-0.5}$ shows better performance. On the other hand,~~ Since the $BAL^{-0.5}$ uses a very low threshold, it classifies more pixels as ~~a convective typethan MRMS in the 14 June 2012 case (Figure 3b), but the results from BAL^0 are more consistent with MRMSoutputs. The overall~~ convective type, and the obtained

R^{CS} ~~from MRMS, SVM, BAL^0,~~ scores are higher than MRMS. In term of CSI, POD, and FAR, SVM and BAL$^{-0.5}$ ~~are shown in Table 1.~~ show similar results, but BAL^0 show apparently worse performance.

To better understand the performance of each approach, the classification results and radar variables (Z, Z_{DR}, and i) from two distinct moments ~~were~~ are examined and shown in Figures ~~4~~5~∼7. ~~Classification~~ Figure 5 shows the classification results from 0303 UTC 30 August 2011~~were first shown in Figure 4~~, where BAL^0, BAL$^{-0.5}$, SVM and MRMS are shown in ~~panel 'a~~the panel 'A', '~~b~~B', '~~c~~C', and '~~d~~D', respectively. The time stamp for the MRMS result is 0300 UTC~~and the time difference from the~~ , and about 3 minutes earlier than the other three approaches~~is about 3 mins~~. These three input variables of SVM at 0303 UTC are shown in Figure ~~5~~6, where Z, Z_{DR}, and i are presented in panel '~~a~~A', '~~b~~B', and '~~c~~C'. From Figures ~~3 and~~ 4 and 5, it could be found that the R^{CS} from MRMS, SVM, and BAL$^{-0.5}$ show similar ~~value~~values, but R^{CS} from BAL^0 is ~~obviously~~ distinctly low. Within the ~~black~~ red circle of Figure ~~5~~6, the averages of Z and Z_{DR} both show relatively large values (Z > 36 dBZ and Z_{DR} > 0.75 dB), this is a clear indication of convective type precipitation. Both SVM and BAL$^{-0.5}$ classify most of the area within the ~~black~~ red circle as convective, and this result is consistent with the MRMS result. Since the separation indexes within the black circle are below or slightly higher than 0, most of the area is classified as stratiform type by BAL^0. For this moment, threshold -0.5 shows better performance than 0.

Figure ~~6 shows the~~ 7 shows another example of classification results from ~~SVM, BAL^0, BAL~~0650 UTC. At this moment, although SVM and BAL$^{-0.5}$ ~~(0801 UTC) and MRMS (0800 UTC)on 14 June 2012. In this case, MRMS, SVM, BAL^0 show similar performance in general, but BAL$^{-0.5}$ shows visible over classification of convective cells. The~~ produce similar CSI (0.30 v.s. 0.25) and POD (0.48 v.s. 0.52), the R^{CS} from ~~MRMS, SVM, and BAL^0 show similar values around 22%, but BAL~~BAL$^{-0.5}$ ~~classifies much more pixels as connective with~~ (32%) is much higher than R^{CS} ~~reaches 41% (Figure 6) . Radar variables are shown in Figure~~ from MRMS (17%) and SVM (13%). These scores could also be found in Figure 4. In Figure 7, ~~and a circle is also inserted in both Figures 6~~ It could be found from that the MRMS, SVM, and BAL$^{-0.5}$ show similar classification results between the azimuthal angle of 180° and ~~7 to emphasize the performance from each approach in this circle. Inside the circle, the echoes with the Z values around 30~35 dBZ have the chances to be either stratiform or convective type~~270°. However, BAL$^{-0.5}$ misclassifies gates between 90° and 180° as convective type, which produces such high R^{CS}. On the other hand, ~~the Z_{DR} shows low value around 0 dB, which is generally considered as the indicator of stratiform~~MRMS and SVM show similar classification results in this region.

3.2.2 Tropical convective

Typhoon Morakot (6∼10 August 2009) brought significant rainfall to Taiwan. Over 700 people were reported dead in the storm, and the property loss was more than 3.3 billion USD. For most of the time during its landfall in Taiwan, the precipitation was classified as a mixture of tropical convective and tropical stratiform types. The performances of SVM, BAL^0, and BAL$^{-0.5}$ were validated ~~with~~ using 96-hour data from 6 to 9 August 2009, where the results from 10 August 2009 were not included in the evaluation because no significant precipitation was observed from that day. The time series plots of R^{CS} ~~,~~(A), CSI (B), POD (C) and FAR (D) are shown in Figure ~~8, demonstrate that the~~ 8. It could be found that scores of R^{CS}, CSI, and POD

from the BAL based approaches is evidently lower than the results from SVM and MRMS, and the latter two show similar performance during ~~this 4-day period~~these four days.

Classification results from BAL^0, $BAL^{-0.5}$, SVM (0402 UTC), and MRMS (0400 UTC) from 9 August 2009 are shown in Figure ~~9a, 9b, 9c, and 9d~~9A, 9B, 9C, and 9D, respectively. The classification results in those regions, highlighted with two circles, are convective (SVM and MRMS) and stratiform (BAL^0 and $BAL^{-0.5}$). Figure 10 includes the reflectivity (~~10a~~A), differential reflectivity (~~10b~~B), and separation index (~~10c~~C) from 0402 UTC, where Figure 10D is the zoom-in reflectivity field inside the ~~reflectivity field within the~~ red rectangular box ~~is shown in Figure 10d~~ (A) for more details. It ~~could~~ was found that the heavy precipitation band is on the top of RCMK (Figure ~~10d~~10D), and this may cause significant attenuation ~~and differential attenuation~~ on Z and Z_{DR} fields. Although both Z and Z_{DR} fields were corrected using Equation 1, deficient or over compensations on Z and Z_{DR} fields lead to increased uncertainty on the separation index. It may be the primary reason causing the small values of the separation index. ~~In Figure 10c~~Other reasons such as wet radome may also contribute to the Z and Z_{DR} issues. In Figure 10C, the separation index i are equal or less than -0.5 in the circled areas, and the BAL based approaches classify these regions as stratiform. On the other hand, these regions clearly show the convective precipitation features in the fields of Z (~~10a~~10A) and Z_{DR} (~~10b~~10D).

3.2.3 Stratiform precipitation event

The performances of BAL^0, $BAL^{-0.5}$, and SVM approaches were also evaluated with a widespread stratiform precipitation event on 26 March 2011. There were no convective type precipitations identified by MRMS, and all these three approaches showed consistent classification results with the MRMS result during an 8-hour period evaluation.

3.3 Sensitivity test

The performances of BAL^0, $BAL^{-0.5}$ and proposed SVM were further validated respecting to the Z_{DR} bias. First, the impact of Z_{DR} bias on i is investigated through a simple simulation. In the simulation, the separation index i is calculated using Equations 2∼5 with four distinct Z values: 10 dBZ, 20 dBZ, 30 dBZ, and 40 dBZ. For each Z value, Z_{DR} changes from -0.5 dB to 2 dB to simulate the Z_{DR} bias. The obtained i results are shown in Figure 11, and the symbol of triangle, diamond, cross, and pentagram indicates the result from 10 dBZ, 20 dBZ, 30 dBZ, and 40 dBZ, respectively. It could be found that for each Z, the calculated i drops when Z_{DR} increases. Moreover, a larger Z produces a larger i for the same Z_{DR} value. As introduced in Section 2.1, the precipitation may be classified as stratiform when i is less than 0. Therefore, positive Z_{DR} calibration bias may result in misclassifying more precipitation as stratiform type.

The impact of the Z_{DR} calibration bias on the performance of BAL^0, $BAL^{-0.5}$, and SVM was investigated using precipitation events from 30 August 2011. In this study, the Z_{DR} filed was first corrected from attenuation, and a ΔZ_{DR} was then manually added on the corrected Z_{DR} field as the artificial bias. The ΔZ_{DR} was set as: -0.2 dB, -0.1 dB, 0 dB, 0.1 dB, and 0.2 dB, respectively. The biased Z_{DR} was calculated as $Z^b_{DR} = Z_{DR} + \Delta Z_{DR}$. The separation index i was calculated using Z^b_{DR} through Equations 2∼5, and classification results from BAL^0 and $BAL^{-0.5}$ were then calculated. The same trained weights and bias vector described in Section 2.3.2 were used in the SVM approach. Following the procedure described in Section 3.2,

scores of R^{CS} (A), CSI (B), POD (C) and FAR (D) are calculated and shown in Figure 12. It should be noted that these scores are the 24-hour averaged values. It could be found that when the ΔZ_{DR} changes from -0.2 dB to 0.2 dB, the R^{CS} from both BAL^0 and $BAL^{-0.5}$ approaches decrease. This indicates that BAL^0 and $BAL^{-0.5}$ classify more precipitation as stratiform, and this results is consistent with the simulation. Both CSI and POD from BAL^0 and $BAL^{-0.5}$ show degradations with the increase of ΔZ_{DR}. On the other hand, the proposed SVM shows slightly better performances when ΔZ_{DR} changes from negative to positive. Both CSI and POD increase when ΔZ_{DR} increases, and the R^{CS} also has the similar trend. One possible reason is that convective type precipitation is normally associated with larger Z_{DR}. As a result, positive ΔZ_{DR} classify more precipitation as convective type. Similar results were also obtained from the case of 6∼10 August 2009.

4 Conclusions

A novel precipitation classification approach using a support vector machine approach was developed and tested on a C-band polarimetric radar located in Taiwan. Different from ~~some existing~~ other classification algorithms that use whole volume scan data, the proposed method only utilizes the data from the lowest unblocked tilt to separate precipitation into convective or stratiform type. It can be applied ~~on~~ to new scanning schemes with more frequent scans at the lowest tilts and lack of information from a higher tilt, such as AVSET, SAILS, MRLE, and etc. Three radar variables of reflectivity, differential reflectivity, and the separation index derived by Bringi et al. (2009) are utilized in the new proposed approach, where both reflectivity and differential reflectivity need be corrected from attenuation and differential attenuation. Although the separation index alone can be used in the precipitation classification, there may be two potential limitations: thresholds and ~~attenuation~~the biases on reflectivity and/or differential reflectivity. Although the threshold ~~0 is proposed to separate convective from stratiform types~~"0" was suggested to be used in separating convective type from stratiform type, it was found that a single threshold may not sufficient for all cases. Other thresholds (such as ~~-0.5~~ "-0.5" used in the current work), sometimes can produce better results than ~~0. The attenuation is the other potential issue~~"0". The biases may come from mis-calibration, attenuation, wet radome, blockage. Although both reflectivity and differential reflectivity should be corrected from attenuation before used in the separation index calculation, the correction biases on either filed may cause large uncertainty in the derived separation index and further lead to a wrong classification. Other factors also may have impacts on the separation index. This work attempts to propose a complementary method to enhance the performance of using the separation index only. The proposed approach integrates input variables with a support vector machine method. The weighs and bias vectors used in the support vector machine were trained with typical stratiform and convective precipitation events. It should be noted that the proposed approach has a flexible framework, and some other variables can be easily included. With newly added variables, the weighting and bias vectors need to be retrained. The proposed approach was tested with multiple cases~~, and its~~. Its performance was found similar to a well-developed approach, MRMS, which utilizes multiple tilts radar data in the classification. It should be noted that the time difference between RCMK (i.e., BAL^0 , $BAL^{-0.5}$, and SVM) and MRMS could be as large as 5 minutes. Therefore, the pixel-to-pixel evaluation criteria of the critical success index (CSI), probability of detection (POD) and false alarm rate (FAR)

may not really reflect their performances. Although a new variable of R^{CS} is used in the performance evaluation, this should be treated as qualitative evaluation.

There are some issues ~~need~~ that need to be noticed before applying this approach into operation. First, this approach is developed for fast scanning and fast update purpose, therefore, ~~only the lowest tilt data~~ data from the lowest unblocked tilt is used as the input. ~~With the higher tilt data as the inputs, potential enhancements should be~~ However, if the radar is located in a complex orography area, radar beam could be partially or completely blocked at some regions. A possible solution for such scenario is using data from different scanning tilts to form a hybrid scan, and the hybrid scan is then used as the input. Radar scanning tilts used in the hybrid scanning are determined by the radar scanning geometry. Given the factor that precipitation's microphysics (such as drop size distribution) from different altitudes may be significantly different, therefore, the performance of proposed approach may be worse than expected. Second, the performance of the proposed approach ~~highly depends~~ depends highly on the training data~~. It should be very careful to select the training data~~, which should be selected very careful. Third, coefficients in the separation index calculation ~~depends~~ depend on the local drop size distribution and drop shape relation features. Therefore, new relations need to be derived for the optimal results. ~~Four,~~ Moreover, the separation index only validates at liquid phase precipitation. For ice phase precipitation, such as mixed hail and rain, its performance is not well studied. Other hydrometeor classification schemes could be used for such scenario. Fourth, this work only presents a prototype algorithm. Given the flexible framework, other variables (such as differential phase) could be easily integrated into this algorithm, and the performance could be further enhanced.

Code and data availability.

The datasets and source code used in this study are available from the corresponding author upon request (yadwang@siue.edu).

Author contributions.

The algorithm was originally developed by Dr. Y. Wang. Dr. L. Tang processed the radar data including generate results from MRMS. Dr. P.-L. Chang and Miss Y.-S. Tang provided and processed radar data from CWB, they were further involved in algorithm discussion and article writing.

Competing interests.

The authors declare that there is no conflict of interest.

Acknowledgements. The authors thank the radar engineers from CWB help us ~~collect~~ collecting and processing the radar data.

References

Adler, R. F. and Negri, A. J.: A satellite infrared technique to estimate tropical convective and stratiform rainfall, J. Appl. Meteor., 27, 30–51, 1988.

Anagnostou, E. N.: Doppler radar characteristics of precipitation at vertical incidence, Rev. Geophys. Space Phys., 11, 1–35, 2004.

Biggerstaff, M. I. and Listemaa, S. A.: An improved scheme for convective/stratiform echo classification using radar reflectivity, J. Appl. Meteor., 39, 2129–2150, 2000.

Bringi, V. N., Chandrasekar, V., Hubbert, J., Gorgucci, E., Randeu, W. L., and Schoenhuber, M.: Raindrop size distribution in different climatic regimes from disdrometer and dual-polarized radar analysis, J. Atmos. Sci., 60, 354–365–2122, 2003.

Bringi, V. N., Williams, C. R., Thurai, M., and May, P. T.: Using dual-polarized radar and dual-frequency profiler for DSD characterization: a case study from Darwin, Australial, J. Atmos. Oceanic Technol., 26, 2107–2122, 2009.

Burges, C. J. C.: A tutorial on support vector machines for pattern recognition, Data Min. Knowl. Discovery, 2, 955–974, 1998.

Capozzi, V., Montopoli, M., Mazzarella, V., Marra, A. C., Panegrossi, N. R. G., Dietrich, S., and Budillon, G.: Multi-variable classification approach for the detection of lightning activity using a low-cost and portable X band radar, Remote Sens., 10, 1797, 2018.

Carey, L. D., Rutledge, S. A., Ahijevych, D. A., and Keenan, T. D.: Correcting propagation effects in C-band polarimetric radar observations of tropical convection using differential propagation phase, J. Appl. Meteor., 39, 1405–1433, 2000.

Chang, W.-Y., Wang, T.-C. C., and Lin, P.-L.: Characteristics of the raindrop size distribution and drop shape relation in typhoon systems in the western Pacific from the 2D video disdrometer and NCU C-band polarimetric radar., J. Atmos. Oceanic Technol., 26, 1973–1993, 2009.

Gourley, J. J., Flaming, Z. L., Vergara, H., Kirstetter, P.-E., Clark, R. A., Argyle, E., Arthur, A., Martinaitis, S., Terti, G., Erlingis, J. M., Hong, Y., and Howard, K.: The FLASH project: improving the tools for flash flood monitoring and prediction across the United States, Bull. Amer. Meteor. Soc., 94, 799–805, 2016.

Grecu, M., Olson, W. S., Munchak, S. J., Ringerud, S., Liao, L., Haddad, Z. S., Kelley, B. L., and McLaughlin, S. F.: The GPM combined algorithm, J. Atmos. Oceanic Technol., 33, 2225–2245, 2016.

Haykin, S. O., ed.: Neural networks and learning machines, Pearson Higher Ed., PP 936, 2011.

Hong, Y., Kummerov, C. D., and Olson, W. S.: Separation of convective and stratiform precipitation using microwave brightness temperature, J. Appl. Meteor., 38, 1195–1213, 1999.

Houghton, H. G.: On precipitation mechanisms and their artificial modification, J. Appl. Meteor., 7, 851–859, 1968.

Houze, R. A. J., ed.: Cloud Dynamics, Academic Press, PP. 573, San Diego, 1993.

Houze, R. L.: Stratiform precipitation in regions of convection: A meteorological paradox?, Bull. Amer. Meteor. Soc., 78, 2179–2196, 1997.

Jameson, A. R.: The effect of temperature on attenuation correction schemes in rain using polarization propagation differential phase shift, J. Appl. Meteor., 31, 1106–1118, 1992.

Kumjian, M. R.: Principles and applications of dual-polarization weather radar. Part I description of the polarimetric radar variables., J. Operational. Meteor., 19, 226–242, 2013.

Leary, C. A. and Jr., R. A. H.: Melting and evaporation of hydrometeors in precipitation from the anvil clouds of deep tropical convection, J. Atmos. Sci., 36, 669–679, 1979.

Park, S. G., Maki, M., Iwanami, K., Bringi, V. N., and Chandrasekar, V.: Correction of radar reflectivity and differential reflectivity for rain attenuation at X-band. part II: evaluation and application, J. Atmos. Oceanic Technol., 22, 1633–1655, 2005.

Penide, G., Protat, A., Kumar, V. V., and May, P. T.: Comparison of two convective/stratiform precipitation classification techniques: radar reflectivity texture versus drop size distribution-based approach, J. Atmos. Oceanic Technol., 30, 2788–2797, 2013.

Powell, S. W., Jr., R. A. H., and Brodzik, S. R.: Rainfall-type categorization of radar echoes using polar coordinate reflectivity data, J. Atmos. Oceanic Technol., 33, 523–538, 2016.

Ryzhkov, A. V. and Zrnic, D. S., eds.: Radar Polarimetry For Weather Observations, Springer Atmospheric Sciences, PP 477, 2019.

Skofronick-Jackson, G. and Coauthors: The global precipitation measurement GPM mission for science and society, Bull. Amer. Meteor. Soc., 98, 1679–1695, 2017.

Smith, T. M., Lakshmanan, V., Stumpf, G. J., Ortega, K. L., Hondl, K., Cooper, K., Calhoun, K. M., Kingfield, D. M., Manross, K. L., Toomey, R., and Brogden, J.: Multi-Radar Multi-Sensor (MRMS) severe weather and aviation products: Initial operating capabilities, Bull. Amer. Meteor. Soc., 97, 1617–1630, 2016.

Steiner, M. and Houze, R. A. J.: Three-dimensional validation at TRMM ground truth sites: Some early results from Darwin, Australia, 26^{th} Int.Conf. on Radar Meteorology, Norman, OK, Amer. Meteor. Soc., pp. 417–420, 1993.

Steiner, M., Jr., R. A. H., and Yuter, S. E.: Climatological characterization of three-dimensional storm structure from operational radar and rain gauge data, J. Appl. Meteor., 34, 1978–2007, 1995.

T., A., Somula, R., K., G., Saxena, A., and A., P.: Estimating rainfall using machine learning strategies based on weather radar data, Int J Commun Syst, p. e3999, https://doi.org/10.1002/dac.3999, 2019.

Testud, J., Bouar, E. L., Obligis, E., and Ali-Mehenni, M.: The rain profiling algorithm applied to polarimetric weather radar, J. Atmos. Oceanic Technol., 17, 332–356, 2000.

Thompson, E. J., Rutledge, S. A., Dolan, B., and Thursai, M.: Drop size distributions and radar observations of convective and stratiform over the equatorial Indian and West Pacific Oceans, J. Atmos. Sci., 72, 4091–4125, 2015.

Tokay, A. and Short, D. A.: Evidence from tropical raindrop spectra of the origin of rain from stratiform versus convective clouds, J. Appl. Meteor., 35, 355–371–4125, 1996.

Vulpiani, G., Montopoli, M., Passeri, L. D., Gioia, A. G., Giordano, P., and marzano, F. S.: On the use of dual-polarized C-band radar for operational rainfall retrieval in mountainous areas, J. Appl. Meteor. Climatol., 51, 405–425, 2012.

Wang, Y., Zhang, J., Ryzhkov, A. V., and Tang, L.: C-band polarimetric radar QPE based on specific differential propagation phase for extreme typhoon rainfall, J. Atmos. Oceanic Technol., 30, 1354–1370, 2013.

Wang, Y., Zhang, P., Ryzhkov, A. V., Zhang, J., and Chang, P.-L.: Utilization of specific attenuation for tropical rainfall estimation in complex terrain, J. of Hydrometeorology, 15, 2250–2266, 2014.

Yang, Y., Chen, X., and Qi, Y.: Classification of convective/stratiform echoes in radar reflectivity observations using a fuzzy logic algorithm, J. Geophys. Res. Atmos., 118, 1896–1905, 2013.

Yen, M., Liu, D., and Hsin, Y.: Application of the deep learning for the prediction of rainfall in Southern Taiwan, Sci. Rep., 9, 12 774, 2019.

Zhang, G., ed.: Weather Radar Polarimetry, CRC Press PP 304, 2016.

Zhang, J., Howard, K., Langston, C., Vasiloff, S., Kaney, B., Arthur, A., Cooten, S. V., Kitzmiller, K. K. D., Ding, F., Seo, D.-J., Wells, E., and Dempsey, C.: National mosaic and multi-sensor QPE (NMQ) system: Description, results, and future plans, Bull. Amer. Meteor. Soc., 92, 1321–1338, 2011.

Zhang, J., Howard, K., Langston, C., Kaney, B., Qi, Y., Tang, L., Grams, H., Wang, Y., Cocks, S., Martinaitis, S., Arthur, A., Cooper, K., Brogden, J., and Kitzmiller, D.: Multi-Radar Multi-Sensor (MRMS) quantitative precipitation estimation: initial operating capabilities, Bull. Amer. Meteor. Soc., 97, 621–638, 2016.

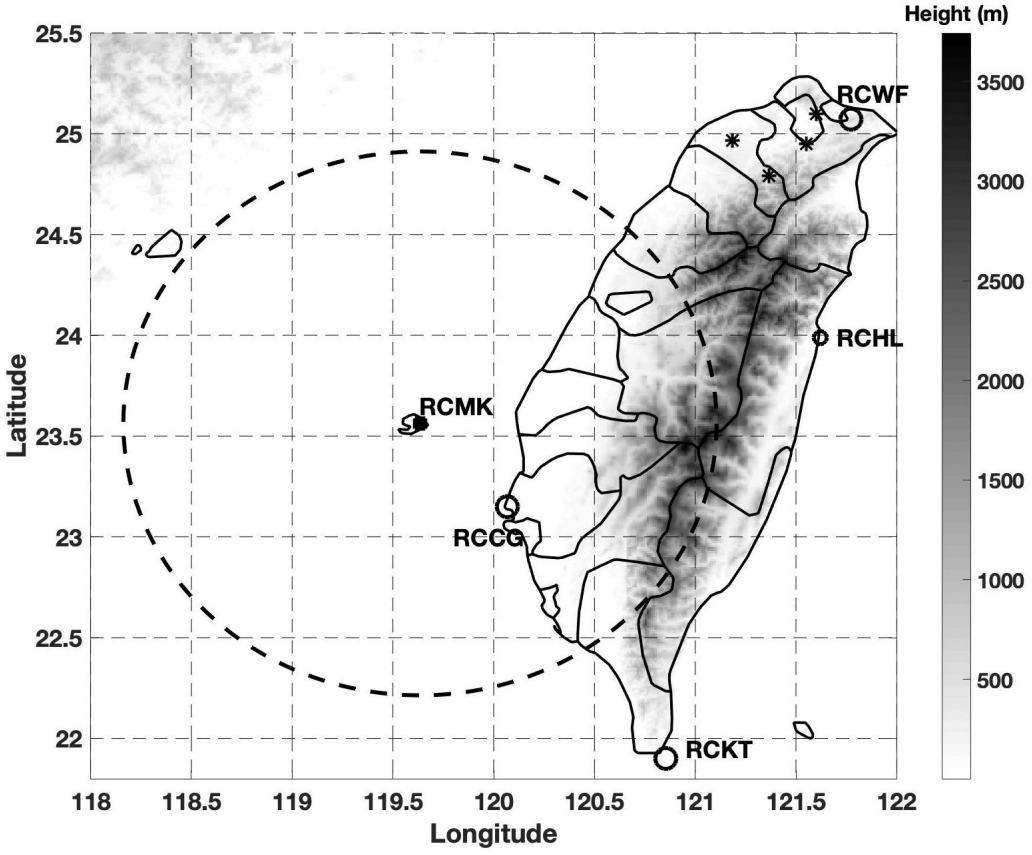

Figure 1. The terrain of Taiwan, the location of a C-band polarimetric radar RCMK (marked with a black square), JWDs (marked with black stars), and four S-band ~~single polarization~~ single-polarization radar RCCG, RCKT, RCHL, and RCWF (marked with black circles). The continuous grey-scale terrain map shows the central mountain range of Taiwan.

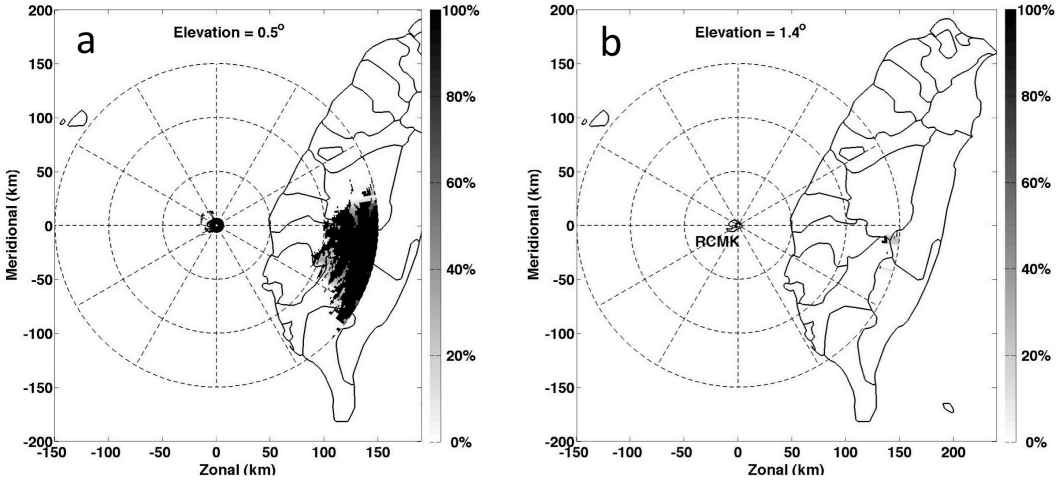

Figure 2. Blockage maps of RCMK from the first 2 EAs (0.5° and 1.4°). The grey scale indicates the blockage percentages.

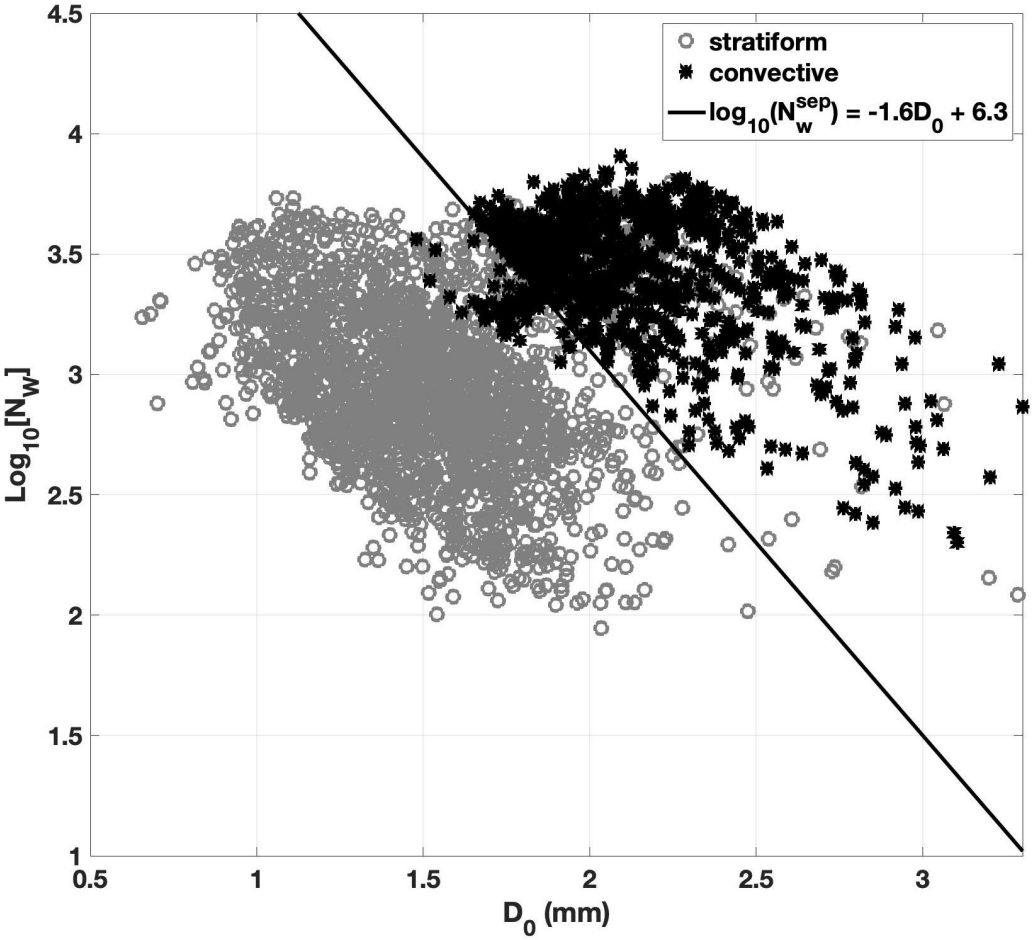

Figure 3. The distribution of $log10(N_w)$ vs D_0. The DSD data from stratiform and convective precipitations are presented with gray circles and black stars, and the separator line is shown with a solid line.

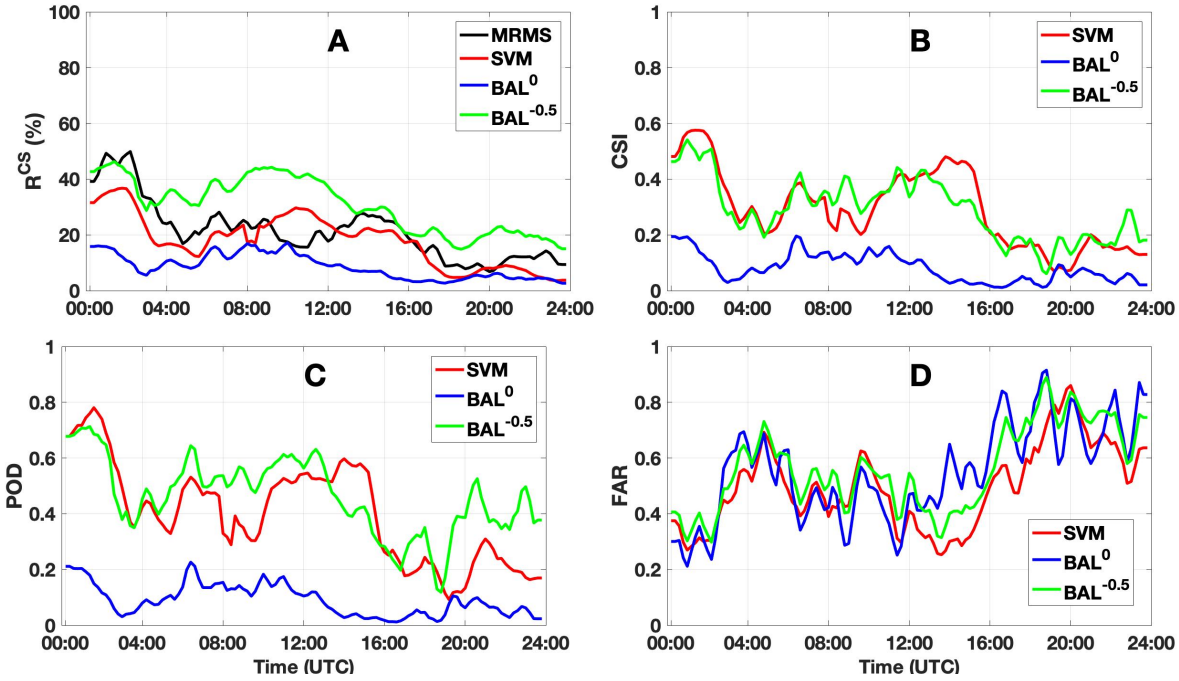

Figure 4. The time series plot of ~~convective cells to stratiform cells ratio (R^{CS}) from 30 August 2011~~ (A)~~and 14 June 2012~~ , CSI(B)~~.~~ , POD(C), and FAR(D) from 30 August 2011. 24-hours data 0000 UTC 2400 UTC are used in each case. The results from BAL with threshold T_0 = -0.5, BAL with threshold T_0 = 0, SVM, ~~and~~ MRMS, are ~~indicated with thin dashed~~presented by green, ~~thin solid~~blue, ~~thick dashed~~ red and ~~thick solid~~ black lines, respectively.

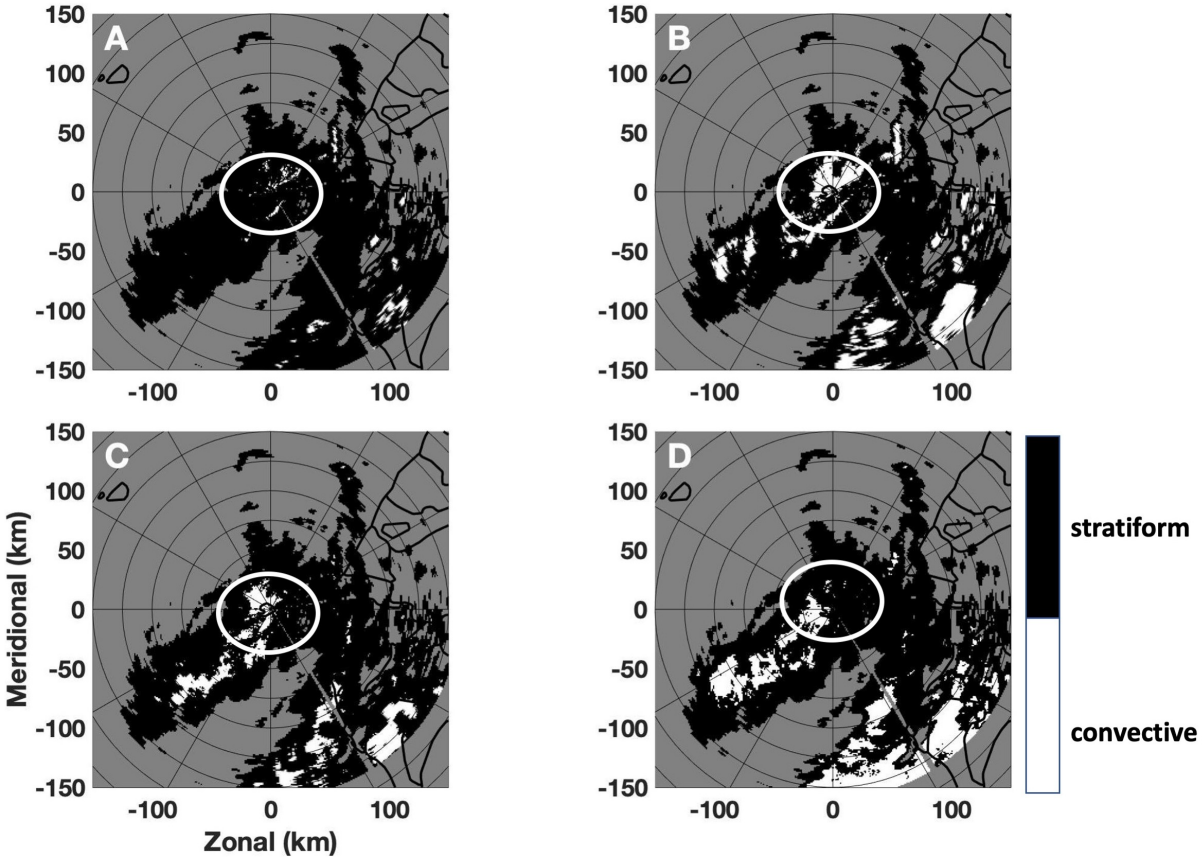

Figure 5. The classification results from BAL^0(~~a~~A), $BAL^{-0.5}$(~~b~~B), SVM(~~c~~C) and MRMS(~~d~~D). The time stamp for BAL^0, $BAL^{-0.5}$, and SVM is 0303 UTC 30 August 2011, and time stamp for MRMS is 0300 UTC 30 August 2011. The region inside the white circle is used in the analysis.

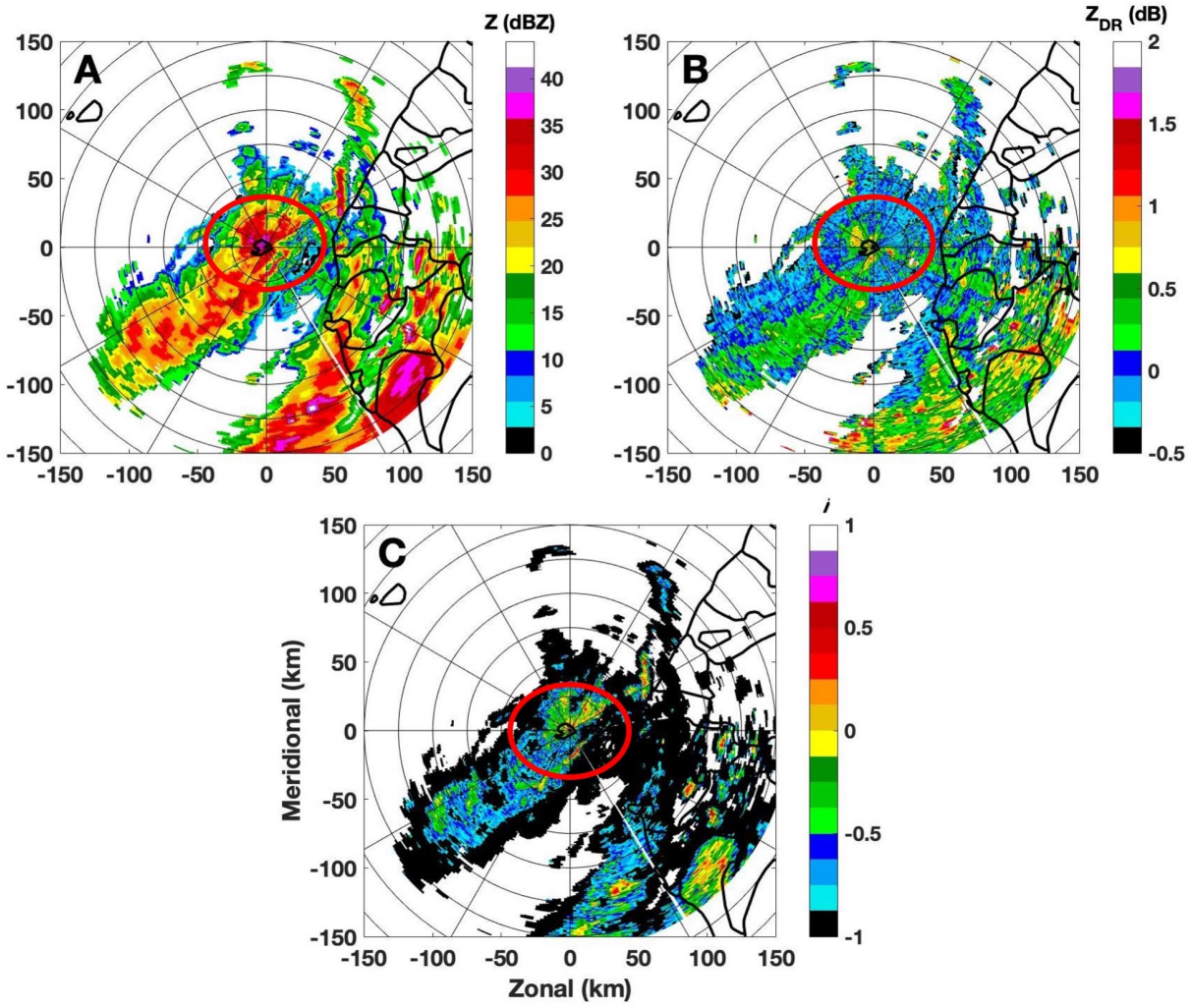

~~Similar to Figure 4~~ The ~~results are from 14 June 2012. The time stamp for BAL^{0}, BAL$^{-0.5}$, and SVM~~ region inside the red circle is ~~0801 UTC, and time stamp for MRMS is 0800 UTC~~used in the analysis.

~~Similar to Figure 4~~ The ~~results are from 14 June 2012. The time stamp for BAL^{0}, BAL$^{-0.5}$, and SVM~~ region inside the red circle is ~~0801 UTC, and time stamp for MRMS is 0800 UTC~~used in the analysis.

Figure 6. Radar variables of reflectivity (~~a~~A), differential reflectivity(~~b~~B), and separation index(~~c~~C). The radar data was collected by RCMK at 0303 UTC 30 August 2011.

~~Similar to Figure 4~~ The ~~results are from 14 June 2012. The time stamp for BAL^{0}, BAL$^{-0.5}$, and SVM~~ region inside the red circle is ~~0801 UTC, and time stamp for MRMS is 0800 UTC~~used in the analysis.

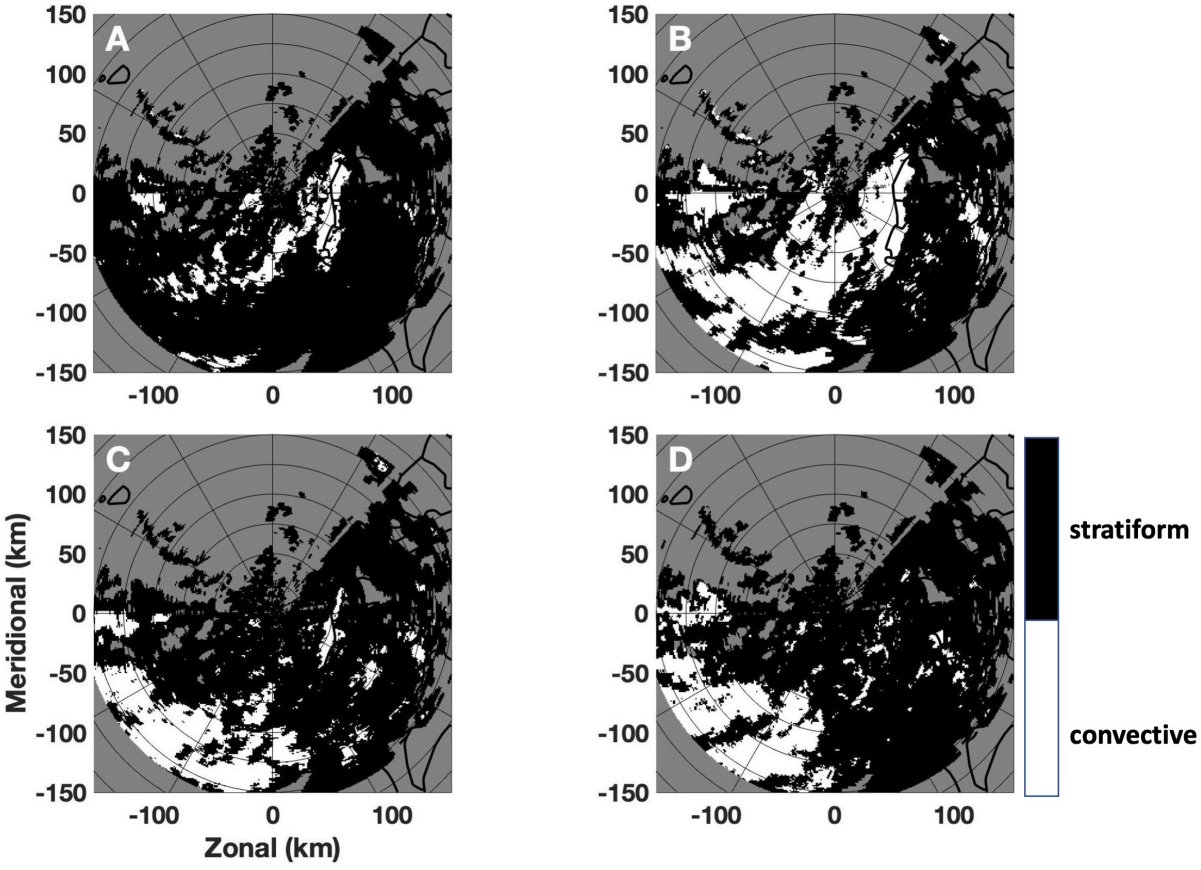

Figure 7. Similar to Figure 5, ~~but radar data~~ results are from ~~0801~~ 0650 UTC~~14 June 2012.~~.

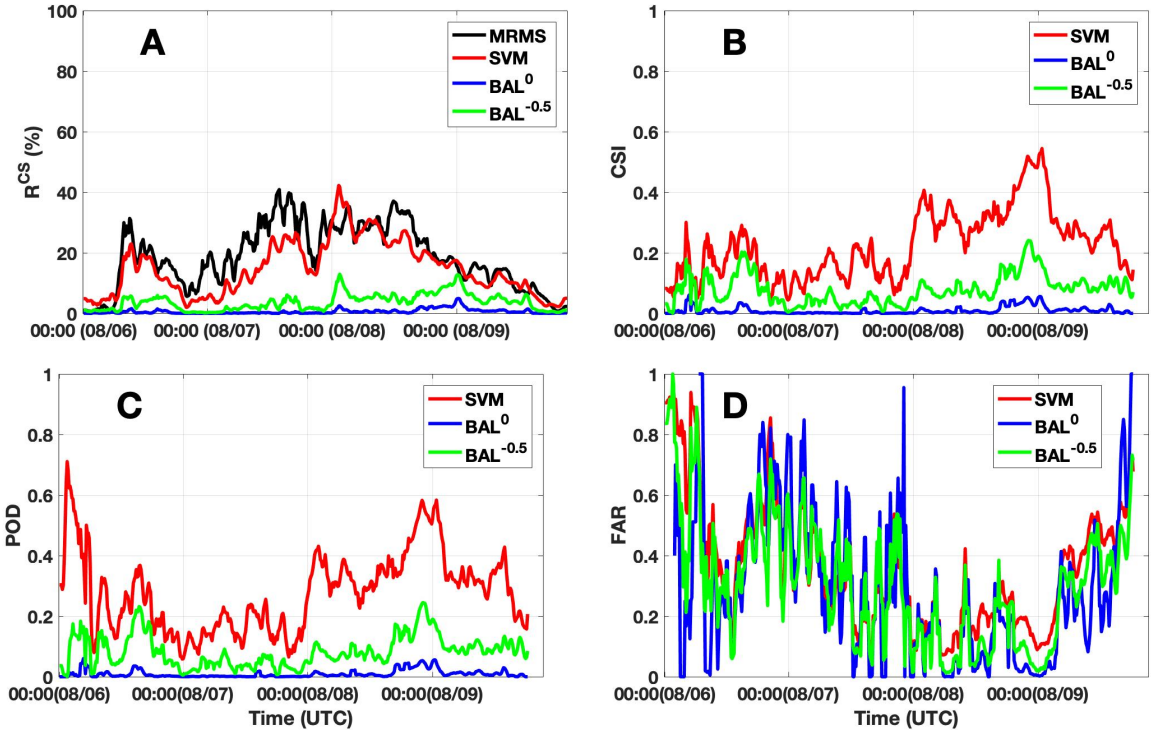

Figure 8. The time series plot of ~~convective cells to stratiform cells ratio~~ R_i^{CS} (~~R~~^{CS}A), CSI(B), POD(C), and FAR(D) from 06~~-~~09 August 2009. 96-hours data are used in each case. The results from BAL with threshold T_0 = -0.5, BAL with threshold T_0 = 0, SVM, and MRMS are indicated ~~with thin dashed~~by green, ~~thin solid~~blue, ~~thick dashed~~ red and ~~thick solid~~ black lines, respectively.

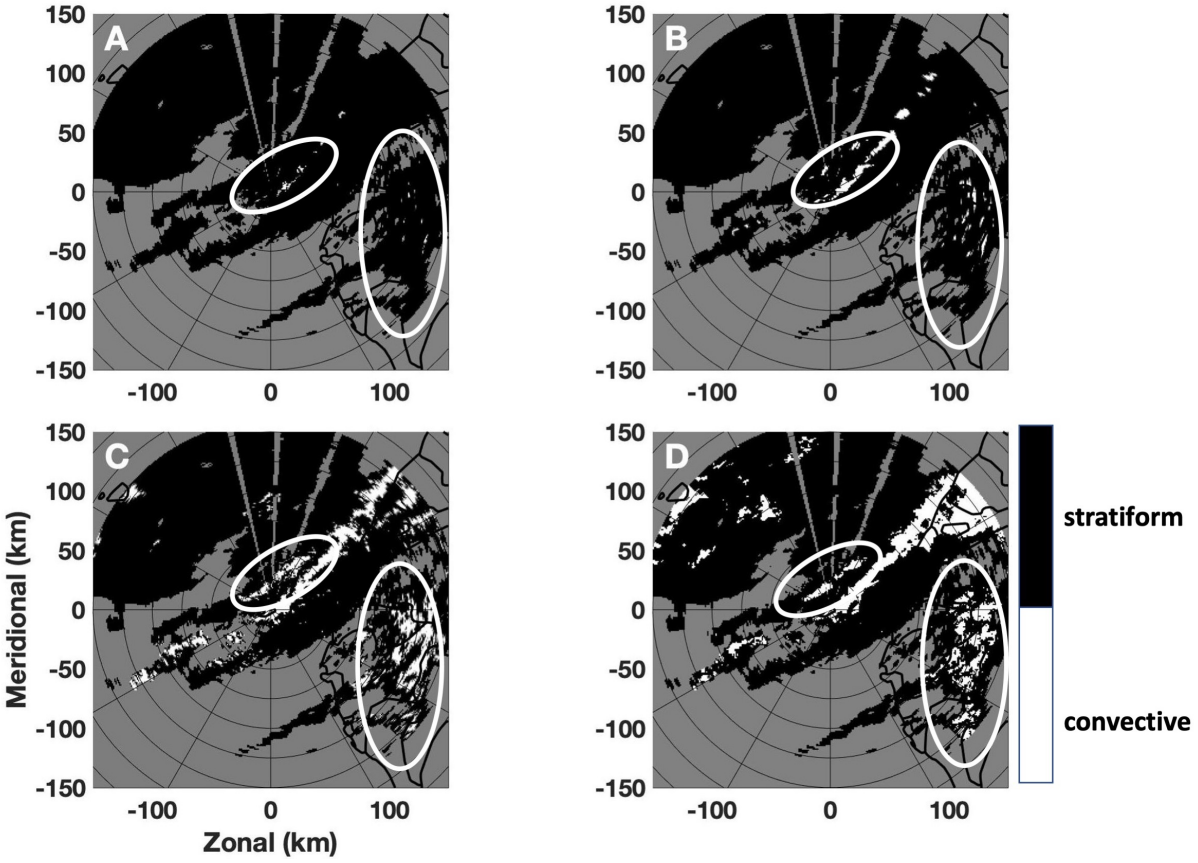

Figure 9. The classification results from BAL^{0}(~~a~~A), BAL$^{-0.5}$(~~b~~B), SVM(~~c~~C), and MRMS(~~d~~D). The time stamp for BAL^{0}, BAL$^{-0.5}$, and SVM is 0402 UTC 9 August 2009, and time stamp for MRMS is 0400 UTC 9 August 2009.

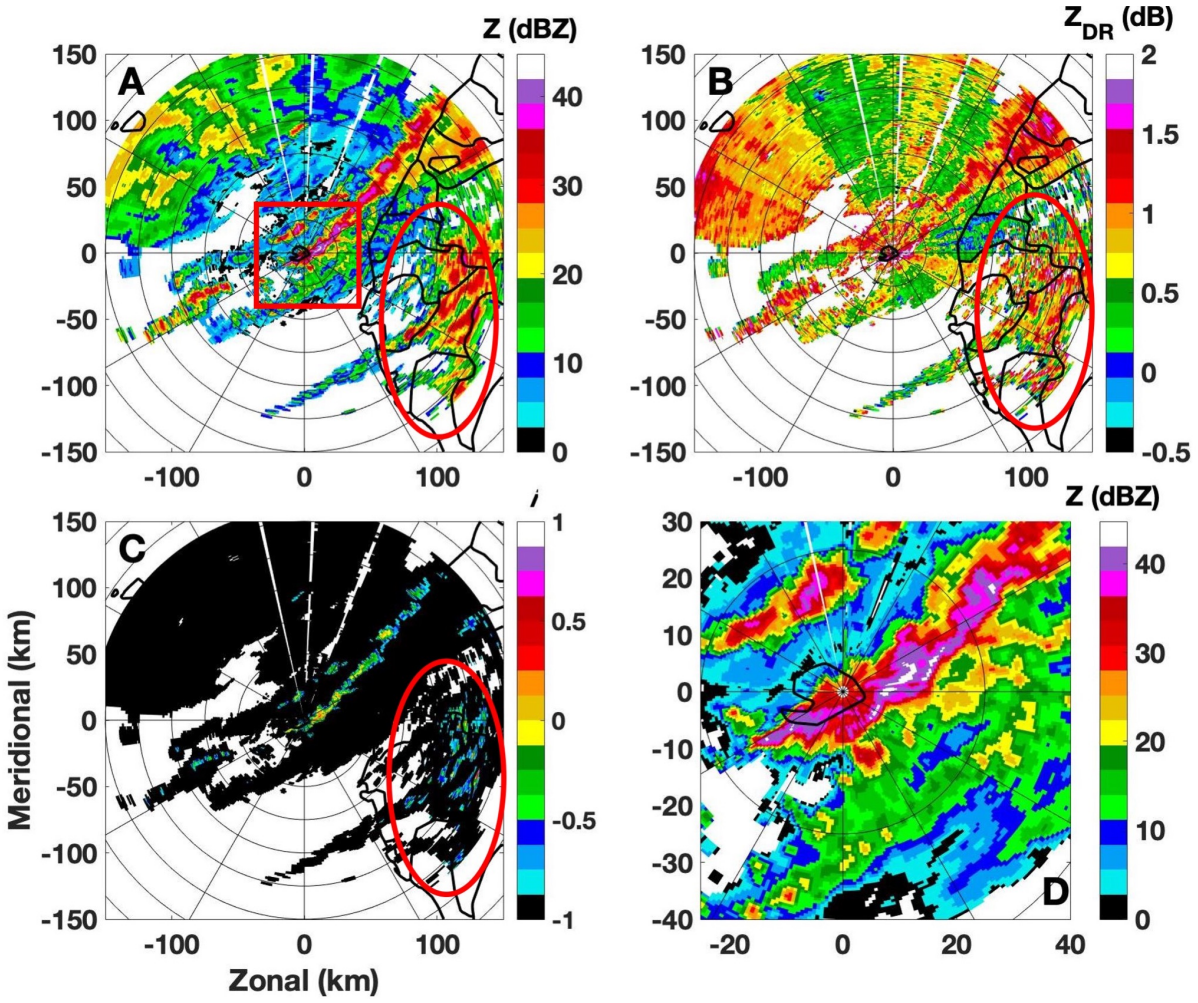

Figure 10. Radar variables of reflectivity(~~a~~A), differential reflectivity(~~b~~B), separation index(~~c~~C), and reflectivity within the red rectangular box in A(~~d~~D). The radar data was collected by RCMK at 0402 UTC 9 August 2009.

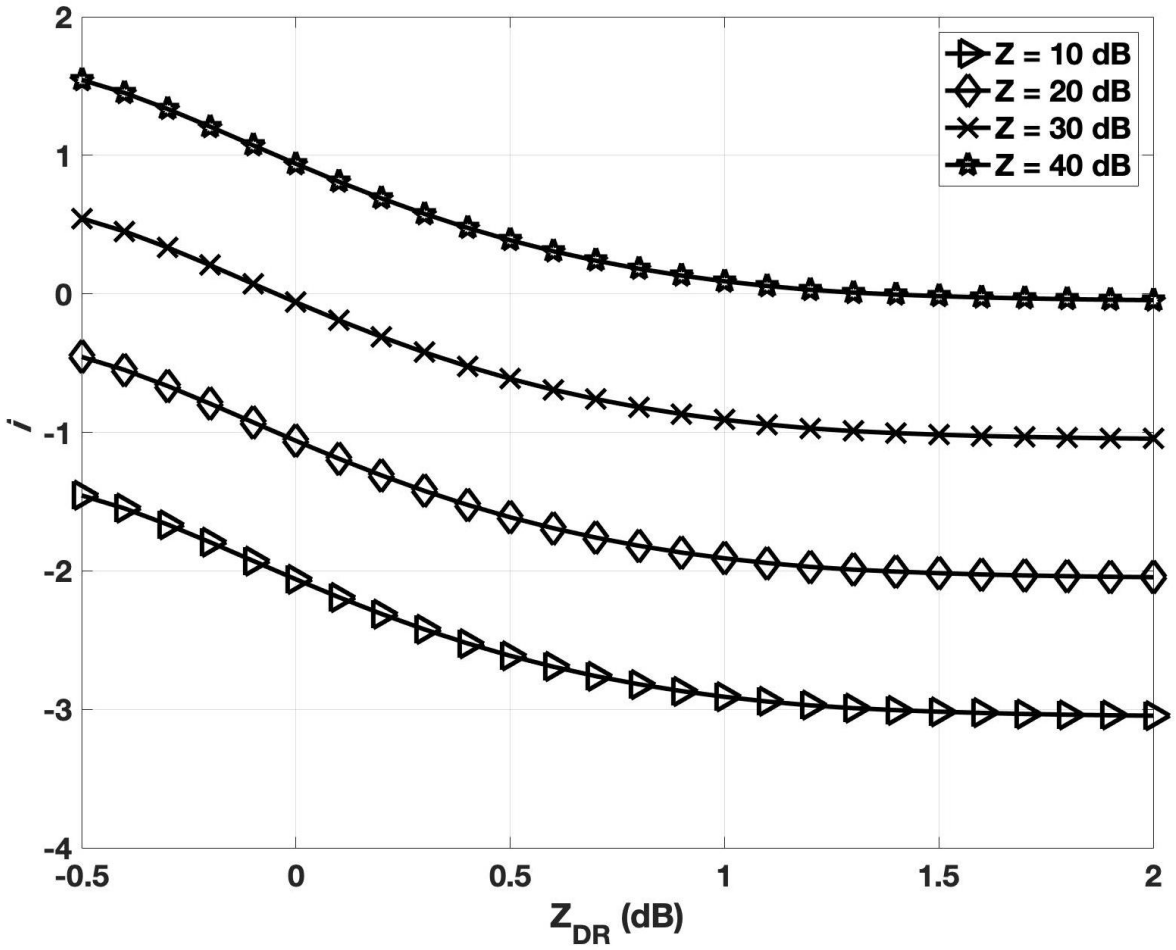

Figure 11. The calculated separation index respecting to different differential reflectivity values.

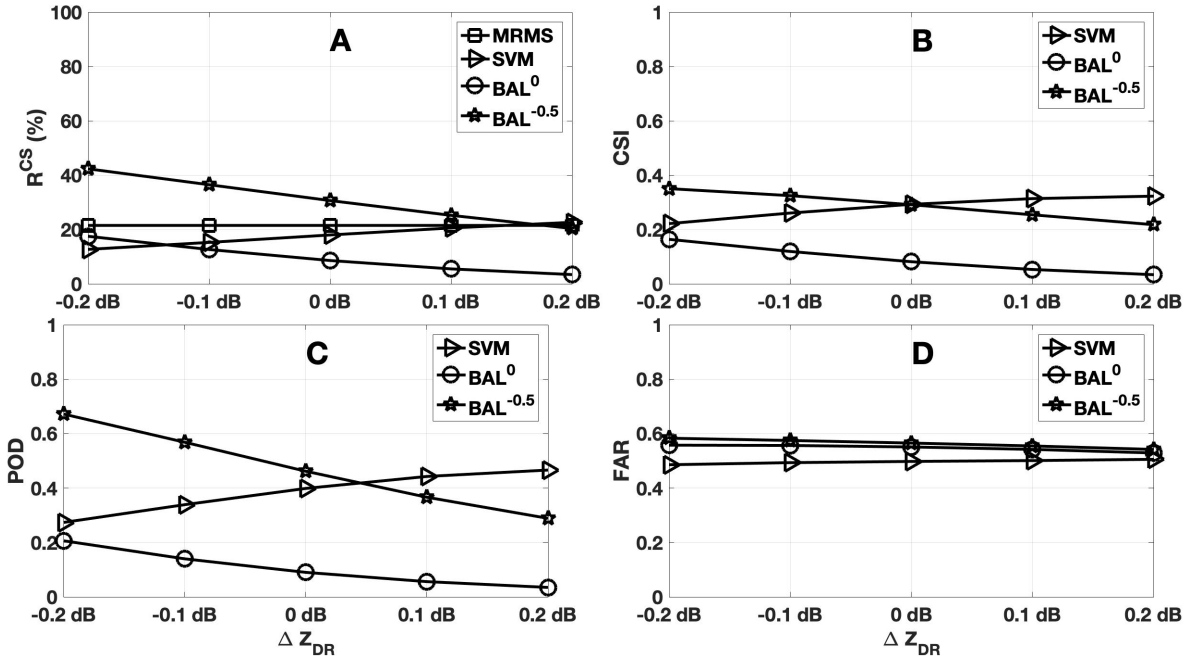

Figure 12. 24-hour averaged R^{CS}(A), CSI(B), POD(C), and FAR(D) from 30 August 2011. The results from BAL with threshold T_0 = -0.5, BAL with threshold T_0 = 0, SVM, and MRMS are indicated with symbols of pentagram, circle, triangle, and square, respectively.

~~The overall performance of these four precipitation events. Case$BAL^0$$BAL^{-0.5}$SVMMRMS30 August 20118%30%19%21%14 June 201215%34%18%20%06~09 August 20091%4%17%22%26 March 20110%0%0%0%Total4.3%12.6%16.6%20.4%~~